The Difunta Correa metasedimentary sequence (NW Argentina): relict of a Neoproterozoic platform? — elemental and Sr-Nd isotope evidence

Carlos Ramacciotti[1,*], César Casquet[2], Edgardo Baldo[1], and Carmen Galindo[2]

[1] *Centro de Investigaciones en Ciencias de la Tierra, Consejo Nacional de Investigaciones Científicas y Técnicas (CONICET), Universidad Nacional de Córdoba, Ciudad Universitaria, 5000 Córdoba, Argentina.*
[2] *Departamento de Petrología y Geoquímica, Instituto de Geociencias, Universidad Complutense, Consejo Superior de Investigaciones Científicas, 28040 Madrid, España.*
** carlosramacciotti@yahoo.com.ar*

ABSTRACT

The Sierra de Pie de Palo (Western Sierras Pampeanas, Argentina) in the Andean foreland is mainly formed by a Mesoproterozoic basement and an Ediacaran metasedimentary cover referred to as the Difunta Correa metasedimentary sequence. The latter is key to understanding the characteristics of this region prior to the early Cambrian assembly of SW Gondwana. It is composed of low- to medium grade metamorphic rocks (metasandstones, mica-schists, Ca-pelitic schists, metaconglomerates, marbles and less abundant amphibolites) that can be grouped into four informal lithostratigraphic units. The chemical composition of these rocks allows to classify the siliciclastic protoliths as shales, Fe-shales and immature sandstones (wackes, sub-litharenites, litharenites and Fe-sandstones). The sediments were derived from an evolved felsic to intermediate continental source and were deposited on a continental passive margin overlaying a Mesoproterozoic basement that crops out at several places of the Western Sierras Pampeanas. Thick marine carbonate beds with seawater isotope composition, phosphatic clasts and the lack of contemporaneous, arc related igneous rocks, also support a passive margin sedimentation. Phosphatic clasts within metaconglomerates are described for the first time in the Sierras Pampeanas and were probably formed after an important Neoproterozoic glaciation (Marinoan). We further suggest, based on our data and previous works, that the passive margin probably belonged to the Paleoproterozoic MARA (acronym of Maz, Arequipa, Río Apa) continental block. MARA, which remained juxtaposed to Laurentia since the middle to late Mesoproterozoic orogenies until its eventual drifting in the late Neoproterozoic, finally accreted to SW Gondwana in early Cambrian times during the Pampean orogeny.

Key words: geochemistry; metasedimentary rocks; neoproterozoic; Western Sierras Pampeanas; phosphatic clasts; Laurentia.

RESUMEN

La Sierra de Pie de Palo (Sierras Pampeanas Occidentales, Argentina), situada en el antepaís Andino, está formada principalmente por un basamento mesoproterozoico y una cubierta metasedimentaria ediacarense. Esta cubierta, denominada secuencia metasedimentaria Difunta Correa, es una unidad clave para entender la paleogeografía de esta región previo al ensamble del suroeste de Gondwana en el Cámbrico inferior. Esta unidad está compuesta por rocas metamórficas de grado bajo a medio (meta-arenitas, esquistos micáceos, esquistos pelíticos cálcicos, metaconglomerados, mármoles y escasas anfibolitas), las cuales pueden agruparse en cuatro unidades litoestratigráficas informales. La composición química de las rocas permite clasificar a los protolitos siliciclásticos como pelitas, Fe-pelitas y areniscas inmaduras (grauvacas, sub-litoarenitas, litoarenitas y areniscas ferruginosas). Los sedimentos se depositaron en un margen continental pasivo y son el resultado de la erosión de una fuente cortical félsica a intermedia, isotópicamente evolucionada. La existencia de potentes capas de carbonatos con composición isotópica de Sr de origen marino, sumado a la presencia de clastos fosfáticos y la falta de rocas ígneas de arco contemporáneas, apoyan la hipótesis de una sedimentación en un margen pasivo sobre un basamento mesoproterozoico que aflora en diversos lugares de las Sierras Pampeanas Occidentales. Se describen aquí, por primera vez, clastos fosfáticos en las Sierras Pampeanas que podrían estar vinculados a una de las principales glaciaciones neoproterozoicas (Marinoense). Además sugerimos, basados en nuestros datos y en trabajos previos, que dicho margen pasivo probablemente formó parte del bloque continental paleoproterozoico MARA (acrónimo de Maz, Arequipa y Río Apa). Este bloque permaneció unido a Laurencia desde las orogénesis del Mesoproterozoico medio y superior, hasta su deriva a fines del Neoproterozoico y acreción al margen suroeste de Gondwana en el Cámbrico inferior (orogenia Pampeana).

Palabras clave: geoquímica de rocas metasedimentarias; neoproterozoico; Sierras Pampeanas Occidentales; clastos fosfáticos; Laurencia.

INTRODUCTION

The Sierra de Pie de Palo (SPP) is one of the Western Sierras Pampeanas (WSP) of Argentina which resulted from Cenozoic uplift in response to shortening of the Andean foreland (Jordan and Allmendiger, 1986; Isacks, 1988). The WSP mainly consists of middle to late Mesoproterozoic basement and a late Neoproterozoic (Ediacaran) sedimentary cover (McDonough *et al.,* 1993; Casquet *et al.,* 2001; Galindo *et al.,* 2004; Rapela *et al.,* 2005). Basement and cover were overprinted by metamorphism and penetrative deformation during the widespread early to middle Ordovician accretionary Famatinian

Ramacciotti, C., Casquet, C., Baldo, E., Galindo, C., 2015, The Difunta Correa metasedimentary sequence (NW Argentina): relict of a Neoproterozoic platform? – Elemental and Sr-Nd isotope evidence: Revista Mexicana de Ciencias Geológicas, v. 32, núm. 3, p. 395-414.

orogeny (Casquet *et al.,* 2001; Mulcahy *et al.,* 2011; van Staal *et al.,* 2011). The metasedimentary succession was recognized and named by Baldo *et al.* (1998) as the Difunta Correa metasedimentary sequence (DCMS) and represents a poorly known Neoproterozoic basin. Likely, the DCMS also crops out in other ranges of the WSP, namely Maz, Espinal and Umango (Figure 1a) where a mesoproterozoic basement has also been recognized (Casquet *et al.,* 2008; Varela *et al.,* 2011). However, the original relationships between the basement and the metasedimentary cover are always oscured by shearing and faulting.

The DCMS constitutes a key entity to the paleogeography of the WSP during the late Neoproterozoic, before its accretion to southwestern Gondwana in the early Cambrian (Casquet *et al.,* 2012; Rapela *et al.*, 2015). These authors suggest that the WSP Mesoproterozoic basement developed after the MARA Paleoproterozoic craton (MARA, acronym of Maz, Arequipa, Río Apa). This craton was accreted to Laurentia -and consequently reworked- in the middle to late Mesoproterozoic orogenies between *ca.* 1.3 and 1.0 Ga. MARA drifted away from Laurentia in the late Neoproterozoic, resulting in the opening of the Iapetus Ocean. This basement was further involved in the early Cambrian Pampean orogeny of the Eastern Sierras Pampeanas by collision with other southwestern Gondwana cratons (such as Kalahari). This collision resulted in the closure of the hypothetical Clymene Ocean (Trindade *et al.,* 2006), and its southeastern extension (present position), *i.e.,* Puncoviscana Ocean.

Conventional petrological provenance studies of detrital rocks (sandstones; Dickinson and Suczek, 1979; Zuffa, 1985; Jonhsson, 1993; Arribas *et al.,* 2007) are hindered if the rocks underwent significant metamorphism and deformation. Primary components of the sedimentary rocks are deeply modified by processes such as recrystallization, formation of new minerals and development of a

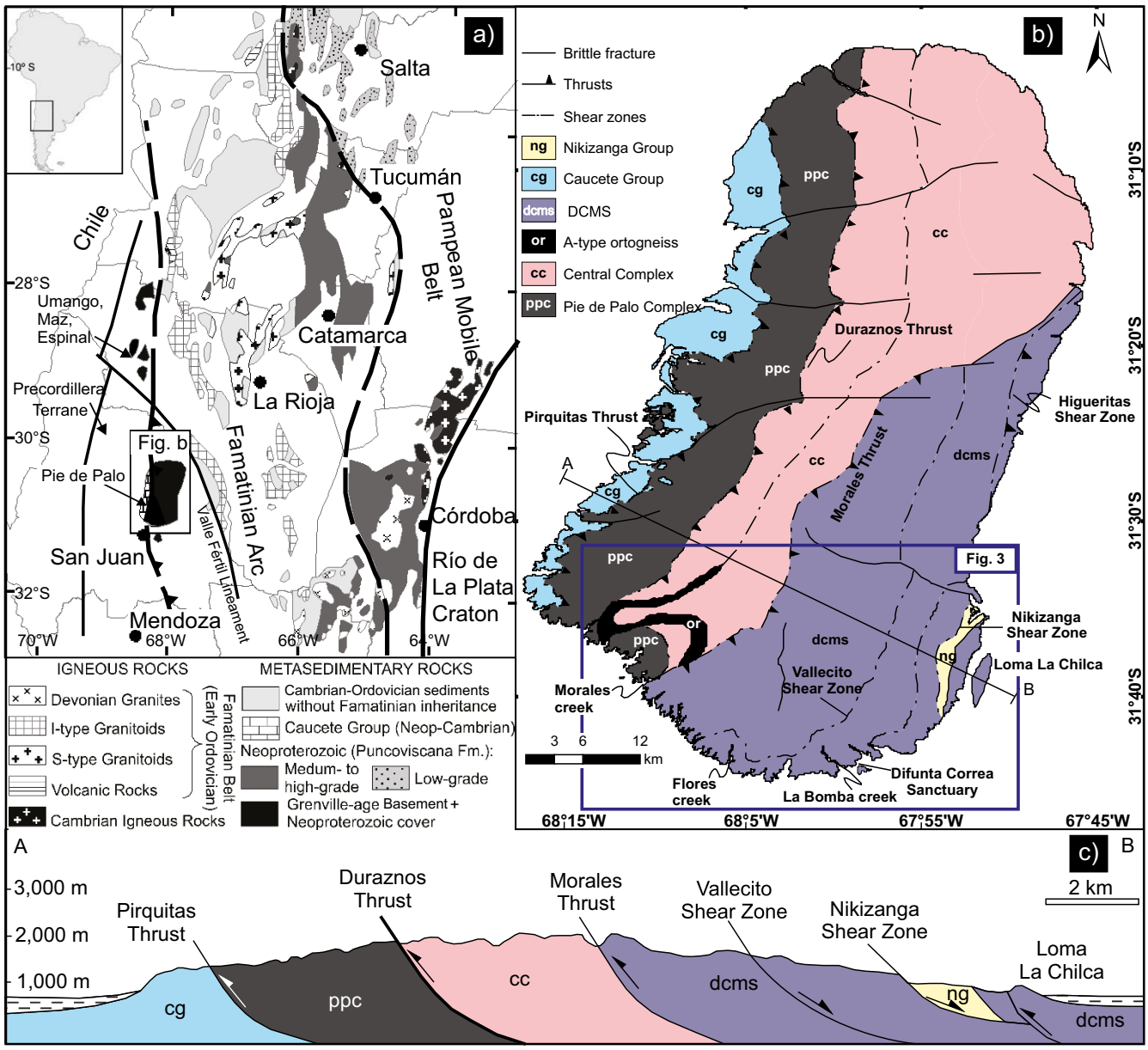

Figure 1. a) Geological setting of the Sierras Pampeanas showing the location of the Sierra de Pie de Palo (SPP); b) Geological map of the SPP; c) Schematic east-west cross-section of the SPP showing the main geological units and structural boundaries. DCMS: Difunta Correa metasedimentary sequence.

new tectonic fabric (foliation). In such cases, methods based on the chemical composition of the metasedimentary rocks help to define the source areas and to establish the tectonic setting of sedimentary basins (Bhatia and Crook, 1986; McLennan *et al.,* 1990, 2003; Zimmermann *et al.,* 2011). However, chemical data alone can lead to erroneous interpretation of the tectonic setting, especially in ancient basins (Armstrong-Altrin and Verma, 2005; Verdecchia and Baldo, 2010). Therefore, they are supported here by complementary evidence from regional geological knowledge and detrital zircon data (Rapela *et al.,* 2015).

Some major and trace elements (*e.g.,* Si, Al, Fe, Mg, Mn, Ca, K, Ba, Sr, Rb and Cs) can be removed from sediments during weathering, diagenesis and low- to medium- grade metamorphism, and therefore they are not appropriate for constraining source areas and/or tectonic settings. On the other hand, elements such as Ti, La, Ce, Nd, Y, Th, Zr, Hf, Nb, and Sc within resistant detrital minerals preserve the initial inter-elemental ratios, and, in consequence, they are useful for provenance analyses (Bhatia and Crook, 1986; Floyd and Leveridge, 1987; McLennan, 1989; McLennan *et al.,* 1990; Zimmermann and Bahlburg, 2003).

The aim of this research is to infer source areas and the tectonic setting of the DCMS through regional, chemical, and isotope evidences of significant rock types, and to discuss the paleogeographic implications. Moreover, we present here the first mention of phosphatic clasts in the Sierras Pampeanas and evaluate their paleoclimatic and paleogeographic significance.

GEOLOGICAL SETTING

The SPP consists of five lithological assemblages bounded by east-dipping shear zones and thrusts. From west to the east they are: the Caucete Group, the Pie de Palo Complex, the Central Complex, the DCMS, and the Nikizanga Group (Figure 1). All these units are overprinted by metamorphism and intruded by igneous rocks, both assigned to the Ordovician Famatinian orogeny (Pankhurst and Rapela, 1998; Casquet *et al.,* 2001; Mulcahy *et al.,* 2011; Baldo *et al.,* 2012).

The Caucete Group (Borrello, 1969; Vujovich, 2003; Galindo *et al.,* 2004; Naipauer *et al.,* 2010; van Staal *et al.,* 2011) is exposed along the western margin of the SPP, in the footwall of the major Pirquitas thrust (Figure 1b), and mainly consists of low- to medium-grade metamorphic rocks such as metasandstones and marbles, and to a lesser extent, metavolcaniclastic rocks. A late Neoproterozoic–early Cambrian depositional age was established for this group based on Sr-isotope composition of marbles (Galindo *et al.,* 2004) and U-Pb zircon ages from metasandstones (Naipauer *et al.,* 2010).

The Pie de Palo Complex (*sensu* Mulcahy *et al.,* 2011) lies between the Pirquitas and the Duraznos thrusts (Figure 1b and 1c) and is mainly composed of ultramafic and mafic rocks, largely metagabbros and garnet-amphibolites. Mesoproterozoic (*ca.* 1,067–1,204 Ma) U-Pb zircon crystallization ages were obtained for this complex (Vujovich *et al.,* 2004; Morata *et al.,* 2010; Rapela *et al.,* 2010; Mulcahy *et al.,* 2011). The Pie de Palo Complex is an igneous sequence formed in a back-arc setting (Vujovich and Kay, 1998).

The Caucete Group and the Pie de Palo Complex have been correlated with the cover and the basement, respectively, of the worldwide known Precordillera terrane. This correlation was based on Sr-isotope composition of marbles (Galindo *et al.,* 2004) and detrital zircon ages (Naipauer *et al.,* 2010) of Caucete Group, and on common Pb composition and geochronology of the ultramafic and mafic rocks of the Pie de Palo Complex (Abbruzzi *et al.,* 1993; Kay *et al.,* 1996). Many authors consider that the Precordillera is an exotic terrane of Laurentian affinity that accreted to the proto-Andean margin during the Famatinian orogeny (Thomas and Astini, 2003; Ramos, 2004).

The Central Complex is defined here as a large block between the Duraznos and the Morales thrusts. The latter ductile thrust was recognized in the Morales creek (Figure 1b) and we were able to track it northward using satellite images. The boundary between the Central Complex and the DCMS is poorly known due to access difficulties. The Central Complex consists of schists, quartzites, marbles, migmatites, amphibolites, metavolcanic rocks and orthogneisses (Casquet *et al.,* 2001; Mulcahy *et al.,* 2011). One orthogneis is an A-type granitoid of *ca.* 774 Ma attributed to the break-up of Rodinia (Baldo *et al.,* 2006). Other orthogneisses range from *ca.* 1,280 to *ca.* 1,027 Ma (McDonough *et al.,* 1993; Rapela *et al.,* 2010; Garber *et al.,* 2014), and therefore, the depositional age of the metasedimentary rocks of this complex has to be older than those of the igneous intrusions. In consequence, the Central Complex probably constitutes a mesoproterozoic basement.

The DCMS was described by Baldo *et al.* (1998) as a sequence made up of metapelites, Ca-pelitic schists, quartzites, quartz-feldspar metasandstones, marbles and para-amphibolites. The DCMS is widespread along the central and eastern parts of the SPP. A late Neoproterozoic depositional age for the DCMS was proposed by Galindo *et al.* (2004) on the basis that the Sr-isotope composition of the calcite marbles corresponds to sea-water composition at that time. The age of, at least, the lower and the middle part of the DCMS probably is *ca.* 600 Ma according to the more recent sea-water compilations and U-Pb detrital zircon ages (Rapela *et al.,* 2005, 2015; Murra *et al.,* 2014). We recognize four units in the DCMS; from bottom to top: La Loma, Flores, Vallecito, and La Bomba (Figure 2).

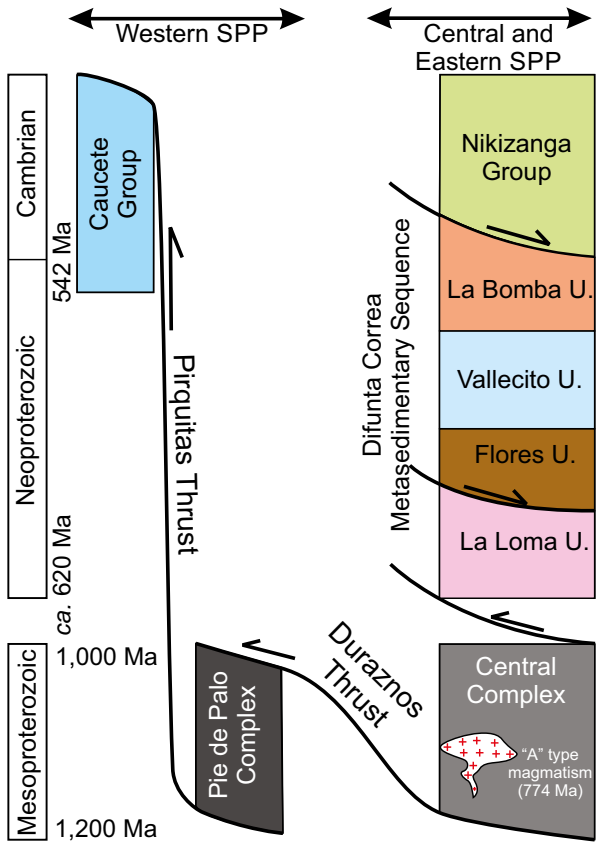

Figure 2. Main units of the Sierra de Pie de Palo (SPP) and structural relationships. Thicknesses are not to scale.

The Nikizanga Group crops out in the southeastern portion of the SPP and consists of low- to medium- grade metamorphic rocks (quartzites, marbles, graphitic schists and, to a lesser extent, amphibolites; Figure 1b). An early Cambrian depositional age was obtained for this group based on Sr-isotope composition of marbles (Filo del Grafito marbles; Galindo *et al.,* 2004), which was latter supported by U-Pb detrital zircon ages from a quartzite (Ramacciotti *et al.,* 2014).

FIELD AND PETROGRAPHIC DESCRIPTIONS

The DCMS was affected by numerous shear zones, thrusts and brittle Andean faults that complicate the overall picture (Figure 3). Sedimentary structures and textures of the DCMS were largely obliterated and replaced by metamorphic textures as a consequence of strong deformation, recrystallization, and formation of new minerals during the Ordovician Famatinian metamorphism (Casquet *et al.,* 2001). Only the metaconglomerates preserve some primary structures (*e.g.,* graded-bedding and cross-bedding) and relict minerals in weakly deformed areas. Thus, the classification of protoliths was mainly based on geochemical data and not on mineral modes. The metasedimentary units are described below, from bottom to top (Figure 4):

La Loma unit consists almost exclusively of black quartz schists and widely outcrops in southeastern SPP (Figure 3). Schists are massive or banded and show a NE-SW striking, east-dipping, penetrative tectonic foliation (Figure 5a). They were affected by numerous shear zones, and often show chevron folds (Figure 5b). The mineral assemblage mainly consists of quartz, with minor amounts of biotite, muscovite, plagioclase and zircon, with a fine-grained (< 1 mm) granoblastic texture (Figure 5c).

The Flores unit consists mainly of metaconglomerates, and less abundant Ca-pelitic schists. The former are matrix-supported with monocrystalline clasts of quartz and feldspar (2–15 mm), and locally, large (5–20 cm) phosphatic clasts which are described below. The metaconglomerates are lens-shaped and often grade in short distances into arenites (Figure 5d). The metamorphic mineral assemblage of the matrix is Qtz-Pl-Bt-Ms±Grt-Ep-Amph-Zrn-Ap-Op (abreviations after Kretz, 1983; Figure 5e and 5f). Phosphatic clasts within the metaconglomerates are between 2 and 20 cm long and were flattened parallel to the main foliation. They consist of Ap-Qtz-Bt-Ilm (identified by electron microprobe) with microgranular texture (Figure 6a and 6b). Internally, the clasts show an alternation of phosphate-rich rock and thin, curved, quartz-rich veinlets (white arrows in Figure 6b). Sometimes an outer zone is found between the phosphatic clasts and the host conglomerate, containing abundant disseminated apatite, probably due to the exchange reaction during metamorphism (zone I in Figure 6a; see Discussion section). The mineral mode of phosphate rock was estimated using the software imageJ (Abràmoff *et al.,* 2004). Sample SPP-22007D1 yielded: 45.5 % Ap, 41.6 % Qtz, 10.2 % Bt, 2.7 % Ilm (Figure 7). Ca-pelitic schists consist of Ms-Hbl-Grt-Bt-Ep-

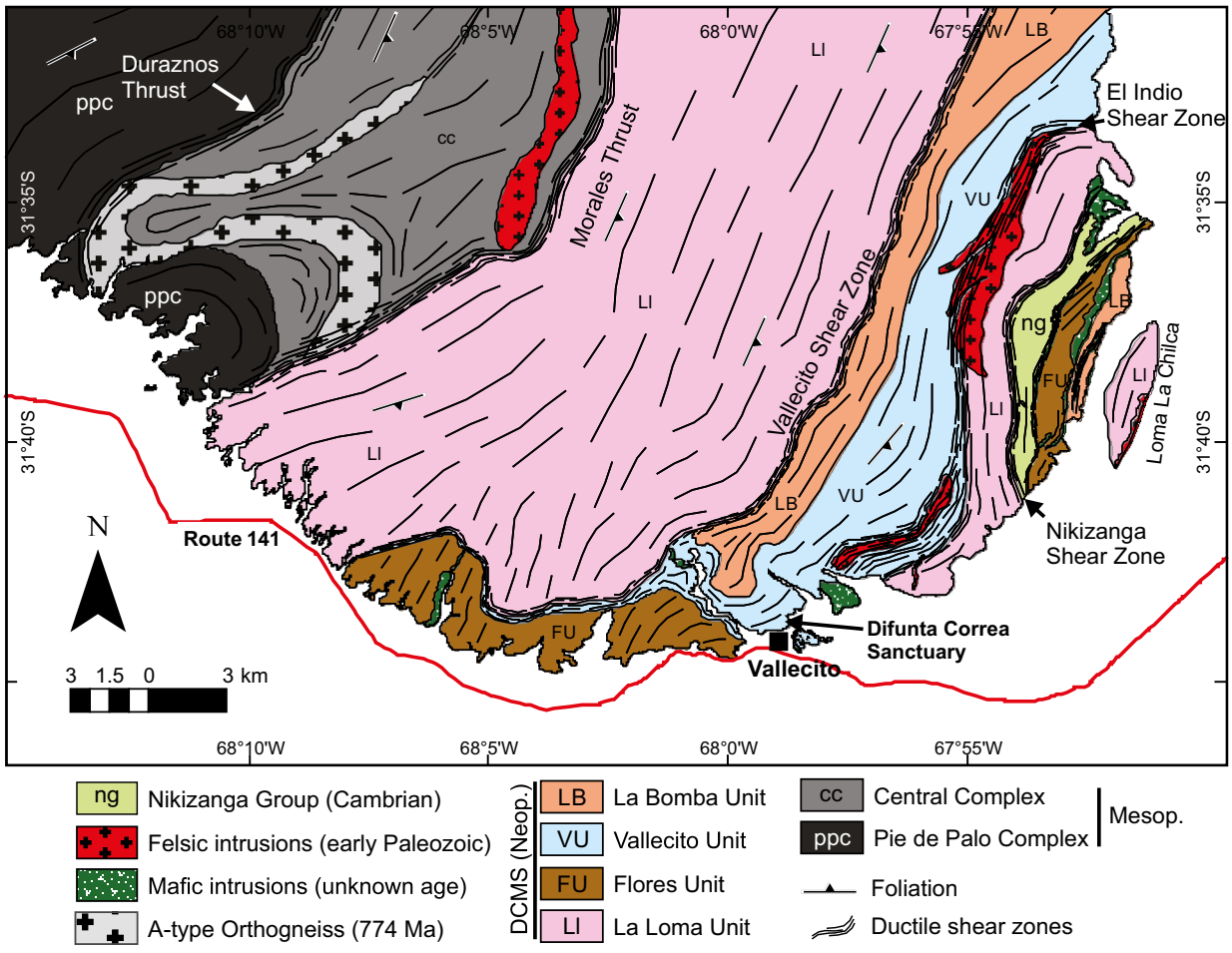

Figure 3. Geological map of the southern SPP showing the four units of the Difunta Correa metasedimentary sequence (DCMS).

Chl-Pl±Zrn-Op. They are characterized by the presence of Ca-minerals (amphibole and/or epidote) in association with typical metapelite minerals (*e.g.,* muscovite, biotite, garnet). Distinctive textural features consist of large, needle-shaped porphyroblasts of hornblende lying in the foliation plane with a radial arrangement (Figure 8a and 8b), and of garnet porphyroblasts discordant to the foliation (Figure 8b). Both textures suggest that minerals grew up late relative to foliation development. The textures and mineral composition of the DCMS Ca-pelitic schists are remarkably similar to *garben*-schists or *garbenschiefer* in the eastern Alps (Selverstone *et al.,* 1984).

The Vallecito unit, with a maximum apparent thickness of 3000 m, is mainly composed of calcite-rich marbles interbedded with calc-silicate rocks and quartzites. An abundant type of calc-silicate rock is para-amphibolite, *i.e.,* amphibolite formed after a sedimentary protolith (Rapela *et al.*, 2005). Marbles are often intruded by Ordovician granitoids (Baldo *et al.,* 2012) (Figure 8c) and exhibit a granoblastic texture with the minerals Cal±Dol-Ms-Bt-Chl-Pl-Qtz-Ttn-Zrn-Ap (Figure 8d).

La Bomba unit is composed of a succession of metapelites and metasandstones of variable composition (Figure 9a). The main rock types are: staurolite-garnet schists, garnet schists, hornblende-garnet metasandstones and calcite-rich metasandstones. The staurolite-garnet schists have a mineral assemblage of St-Grt-Bt-Ms-Pl-Qtz±Ap-Zrn and are characterized by the abundance of staurolite and garnet porphyroblasts set in a foliated mica-rich matrix (Figure 9b and c). The garnet schists consist of Ms-Grt-Bt-Qtz-Pl also with garnet as porphyroblasts and a lepidoblastic to granoblastic matrix (Figure 9d). The hornblende-garnet metasandstones bear many similarities to Ca-pelitic schists (garben-schists) of the Flores unit, whit the exception that they are more psammitic (Figure 10a-10c; compare with Figure 8a). The calcite-rich metasandstones are mainly composed of quartz and calcite, whit minor amounts of muscovite, and show a granoblastic texture (Figure 10d).

SAMPLING AND ANALYTICAL METHODS

Representative samples from the three meta-detrital units that form the DCMS were chosen for chemical and isotope analyses. Details of each sample are given in Table 1.

Chemical analyses were carried out on eleven samples (Table 2). Six samples were analyzed at Activation Laboratories Ltd. (Actlabs, Ontario, Canada) following the 4 Litho-research routine. Major elements were determinate by ICP-AES, whereas minor and trace elements were determinate by ICP-MS. The remaining five samples were analyzed by X-ray fluorescence (XRF) at the Laboratorio of the Instituto de Geología y Minería, Universidad Nacional de Jujuy, Argentina on a Rigaku FX2000 spectrometer with Rh tube (Table 2). Ground and homogenized samples were fused with lithium tetraborate for major element analyses. Trace element determinations were performed on rock powder pellets mixed with methyl methacrylate, and pressed at 20 t. Operating conditions were 50 *kV* and 45 *mA*.

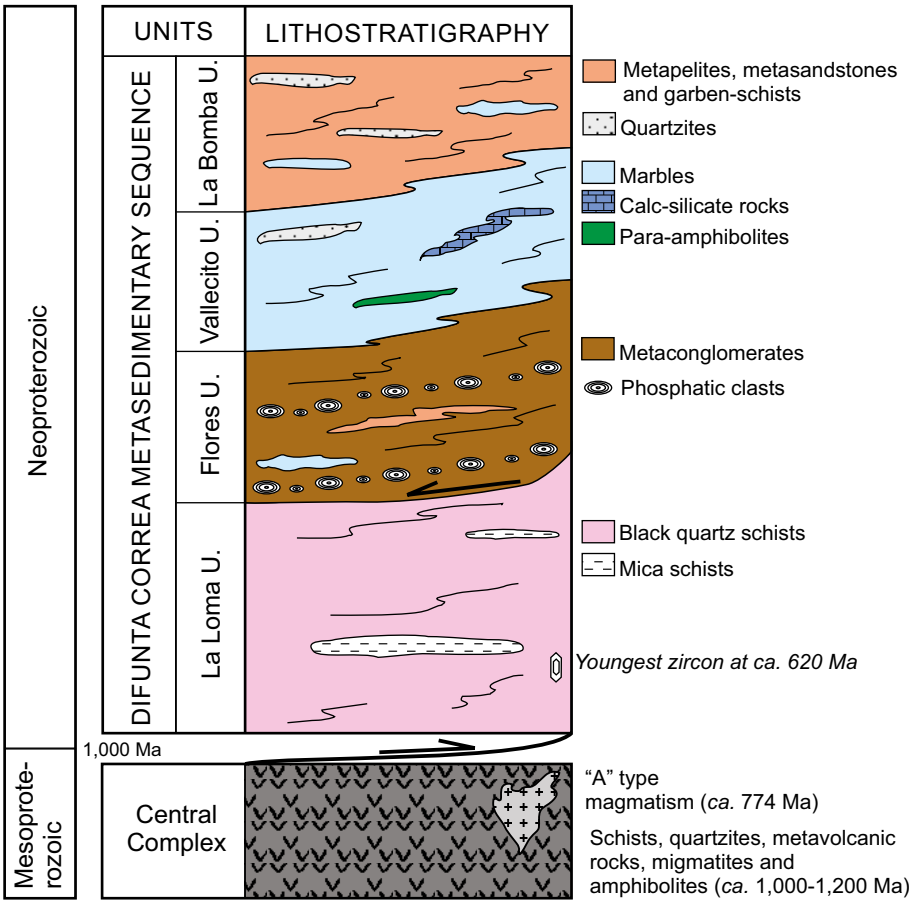

Figure 4. Schematic lithostratigraphic column of the Difunta Correa metasedimentary sequence. The youngest zircon age is from Rapela *et al.* (2005, 2015).

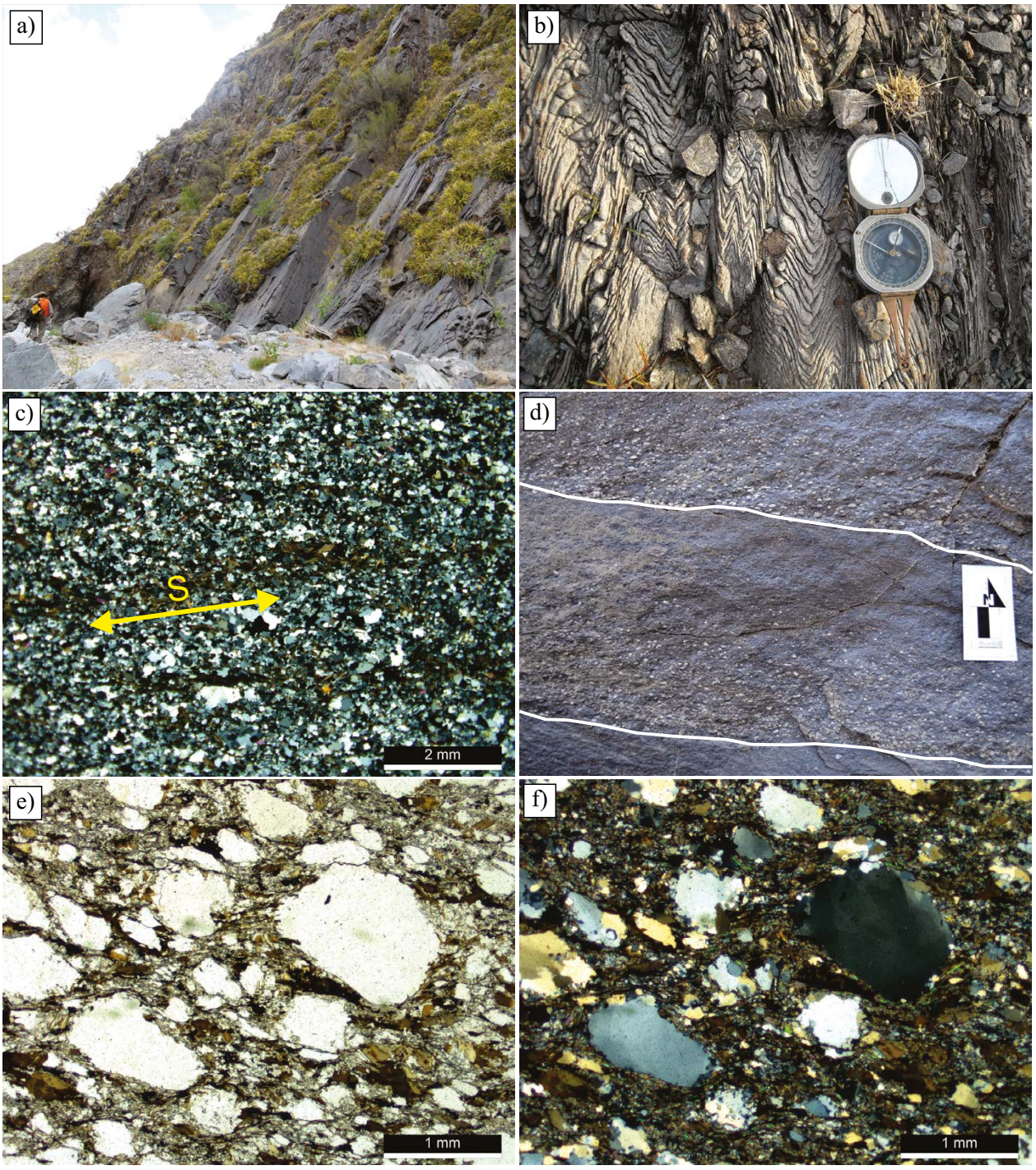

Figure 5. Field and petrographic characteristics of La Loma unit (a-c) and the Flores unit (d-f). a) Evenly foliated, black, quartz schists; b) Banded and folded (chevron folds) quartz schists; c) Fine-grained granoblastic texture mainly composed of quartz and, to a lesser extent, of oriented micas which define the foliation of the rock; d) Normal graded bedding in metaconglomerates; e) and f) PPL and crossed polars photomicrograph of metaconglomerates showing relict minerals (clasts) and recrystallized matrix.

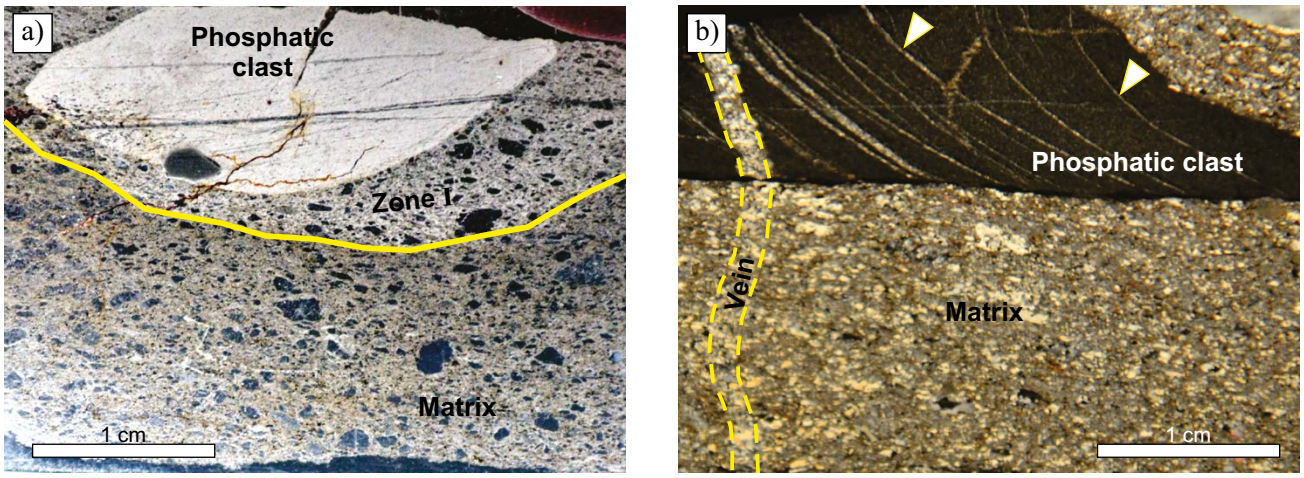

Figure 6. Phosphatic clasts within metaconglomerates of the Flores unit. a) Thin section of one phosphatic clast showing an outer zone of apatite-enriched host conglomerate (zone I); b) Crossed polars photomicrograph of a phosphatic clast with a truncated alternation of phosphate-rich rocks and thin veinlets of quartz (white arrow) and a cross-cutting quartz vein.

Rb-Sr and Sm-Nd isotope analyses were carried out on four detrital rocks. Additionally, Rb-Sr isotope data was collected from two phosphatic clasts within the metaconglomerates of the Flores unit (Table 3). Analytical work was carried out at the Centro de Geocronología y Geoquímica de Isótopos of the Universidad Complutense de Madrid on a PHOENIX© automated multicollector mass-spectrometer. Whole rocks (siliciclastic rocks) were first decomposed in 4 ml HF Merck-suprapure and 2 ml HNO_3 Merck-suprapure in Teflon digestion bombs for 48 hours at 120 ºC, and finally in 6M HCl. Concentrations of Rb and Sr, as well as Rb/Sr atomic ratios, were determined by X-ray fluorescence spectrometry at the X-Ray Centro de Difracción de la Universidad Complutense following the methods of Pankhurst and O`Nions (1973). Sr and REE were separated using Bio-Rad AG50 x 12 cation exchange resin. The phosphatic clasts were decomposed in 6M HCl in Nalgene beakers and, after evaporation, dissolved with 3M HNO_3; Sr was separated using an extraction chromatographic SrResinTM. Errors are quoted throughout as two standard deviations (2σ) from measured or calculated values. The decay constant used in the calculations is $\lambda^{87}Rb = 1.42\times10^{-11}$ year^{-1} recommended by the IUGS Subcommision for Geochronology (Steiger and Jäger, 1977). Bulk Earth Sr-isotope composition was calculated from Allègre *et al.* (1983) and Taylor and McLennan (1985). Analytical uncertainties are estimated to be 0.01 % for $^{87}Sr/^{86}Sr$ and 1 % for $^{87}Rb/^{86}Sr$ ratios. Epsilon-Sr (εSr) values were calculated relative to a Bulk Earth present-day $^{87}Sr/^{86}Sr$ value of 0.7045 and $^{87}Rb/^{86}Sr$ of 0.0827 (DePaolo, 1988). Replicate analyses of the NBS-987 Sr-isotope standard yielded an average $^{87}Sr/^{86}Sr$ ratio of 0.710245 ± 0.00003 (n = 14), (accepted value: 0.71025 ± 0.00005; Faure, 2001)

Samarium and neodymium were determined by isotope dilution using spikes enriched in ^{149}Sm and ^{150}Nd and were separated from the REE group using Bio-beads coated with 10 % HDEHP. Errors are quoted throughout as two standard deviations (2 σ) from measured or calculated values. The decay constants used in the calculations are the values $\lambda^{147}Sm = 6.54\times10^{-12}$ year^{-1} recommended by the IUGS Subcommision for Geochronology (Steiger and Jäger, 1977). Analytical uncertainties are estimated to be 0.006 % for $^{143}Nd/^{144}Nd$ ratios and 0.1 % for $^{147}Sm/^{144}Nd$ ratios. Epsilon-Nd (εNd) values were calculated relative to a present-day chondrite $^{143}Nd/^{144}Nd$ value of 0.512638 and

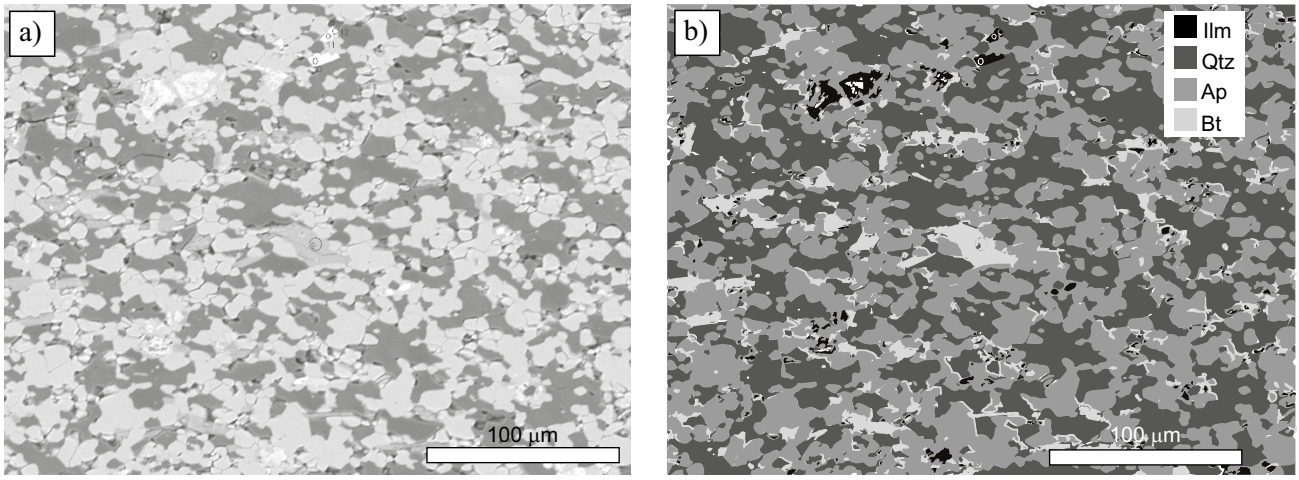

Figure 7. a) Secondary electron (SEM) image showing the slightly orientated microgranular texture of a phosphatic clast core (SPP-22007D1). The black areas are holes which were not considered for modal analysis, and are merged with quartz in b); b) Image a) processed with ImageJ software.

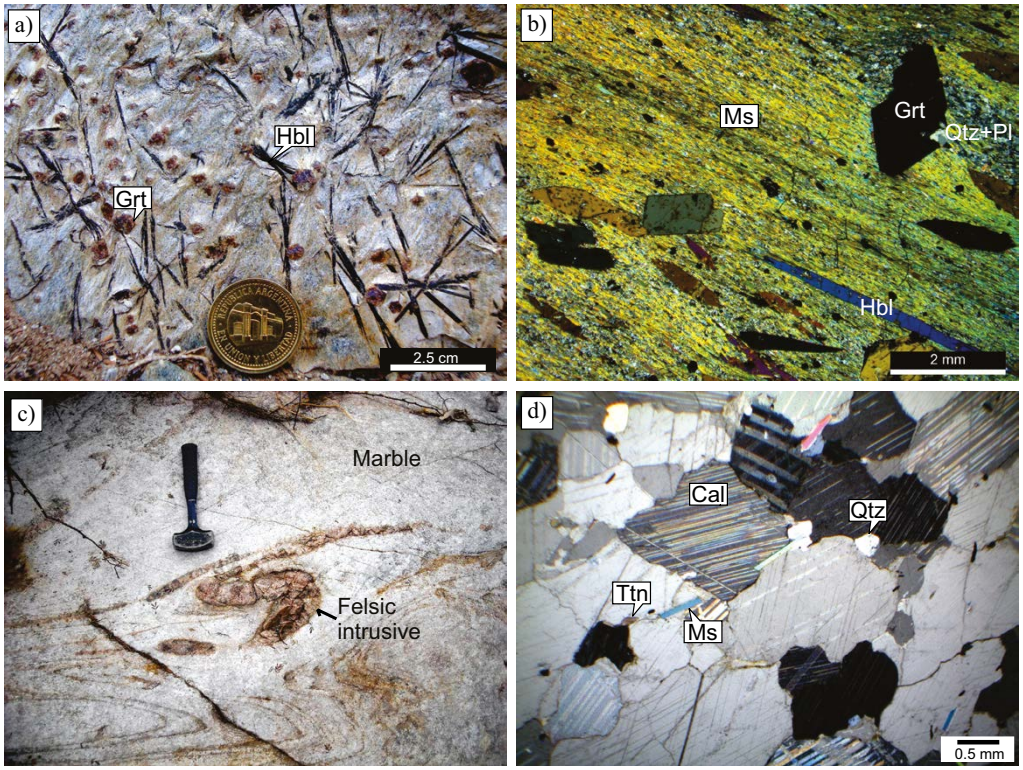

Figure 8. a) and b) Ca-pelitic schists (garben-schists) from the Flores unit. c) and d) Marbles from the Vallecito unit. c) Deformed marble with folded felsic intrusive, d) Crossed polars photomicrograph of marbles showing a granoblastic texture.

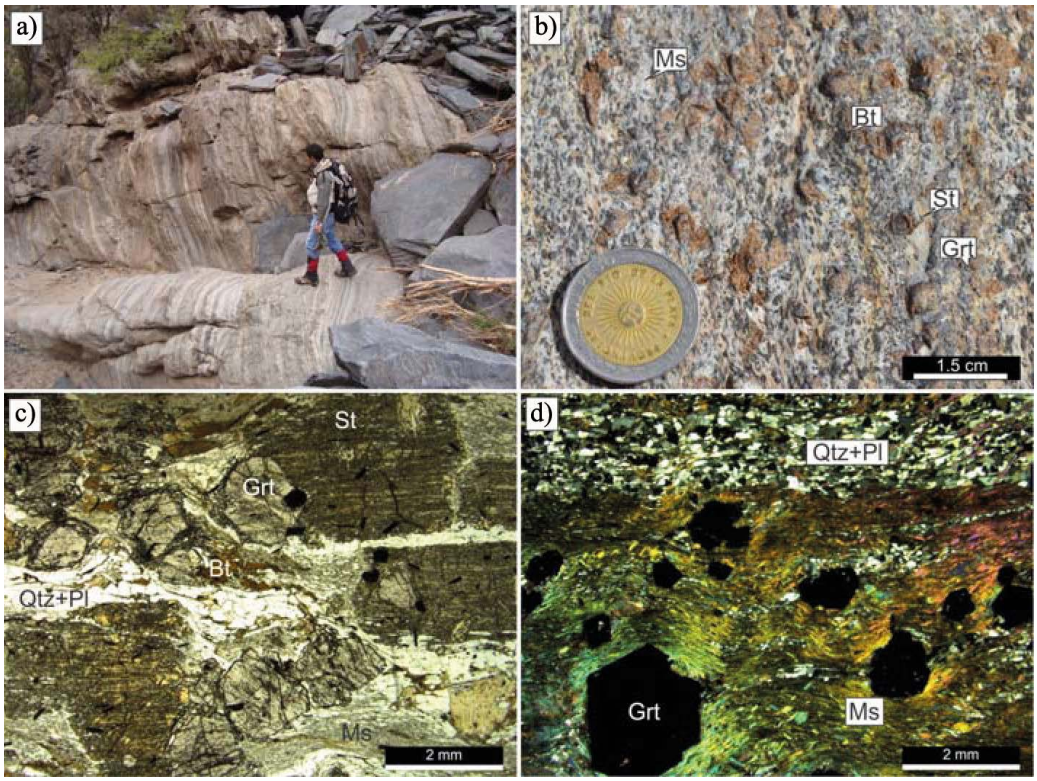

Figure 9. La Bomba unit. a) Succession of metapelites and metasandstones; b) Staurolite-garnet schist; c) PPL photomicrograph of a staurolite-garnet schist; d) Crossed polars photomicrograph of a garnet schist.

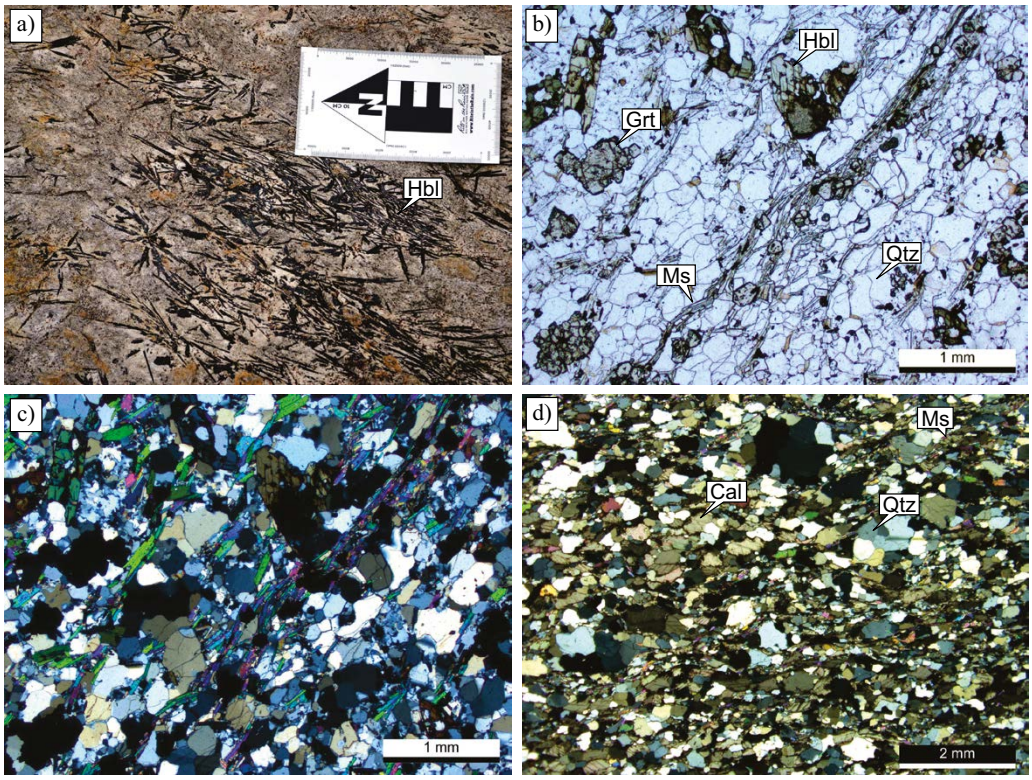

Figure 10. La Bomba unit. a) Hornblende-garnet metasandstone with non-oriented hornblende prisms, locally displaying a radial arrangement; b) and c) PPL and crossed polars photomicrograph of a hornblende-garnet metasandstone; d) Crossed polars photomicrograph of a calcite-rich metasandstone.

$^{147}Sm/^{144}Nd$ of 0.1967 (Jacobsen and Wasserburg, 1980; Goldstein *et al.,* 1984). Eight analyses of La Jolla Nd-standard measured during sample analysis gave a mean $^{143}Nd/^{144}Nd$ ratio of 0.511845 ± 0.00001 (accepted value: 0.511858 ± 0.00007; Lugmair and Carlson, 1978). Single stage model ages (T_{DM}) was calculated according to DePaolo (1988).

The composition of phosphate minerals was determined in one phosphatic clast (SPP-22007D1; Table 4) using a JEOL JXA8230 Superprobe at the Universidad Nacional de Córdoba, Argentina. Carbon-coated polished sections were analyzed at 15 *kV* using 20 *nA* beam and a range of natural and synthetic standards.

RESULTS

Detrital rocks geochemistry

Geochemical data from the DCMS siliciclastic rocks are shown in Table 2. According to Herron´s (1988) plot (Figure 11) the samples are classified as pelites (shales and Fe-Shale) and sandstones (wackes, sub-litharenites, litharenites and Fe-sandstones). The Ca-pelitic schist from the Flores unit shows the lowest concentration of SiO_2 (40.3–46.4 %) and the highest contents of Al_2O_3 (26.2–28.9 %) and K_2O (6.6–7.2 %). Metapelites from La Bomba unit (staurolite-garnet

Table 1. Location and description of the analyzed samples. Mineral abbreviations after Kretz (1983).

Sample	Lat. (S)	Long. (W)	Unit	Rock type	Mineral assemblage
SPP-22013	31° 42′ 24′′	68° 01′ 00′′	La Bomba	Calcite-rich metasandstone	Qtz-Pl-Kfs-Cal-Ms
SPP-27000	31° 34′ 46′′	67° 52′ 51′′	La Bomba	Hornblende-garnet metasandstone	Grt-Hbl-Ms-Bt-Qtz-Pl
SPP-27001	31° 34′ 46′′	67° 52′ 51′′	La Bomba	Mica schist	Grt-Ms-Bt-Qtz-Pl
SPP-27002	31° 34′ 46′′	67° 52′ 51′′	La Bomba	Staurolite-garnet schist	St-Grt-Ms-Bt-Qtz-Pl
SPP-27003	31° 34′ 46′′	67° 52′ 51′′	La Bomba	Quartz schist	Qtz-Ms-Bt-Grt
SPP-424	31° 22′ 55′′	67° 58′ 42′′	La Bomba	Garnet gneiss	Grt-Bt-Ms-Qtz-Pl
SPP-22007D1	31° 43′ 36′′	68° 06′ 00′′	Flores	Phosphatic clast	Ap-Qtz-Bt-Ilm
SPP-22007C1	31° 43′ 36′′	68° 06′ 00′′	Flores	Phosphatic clast	Ap-Qtz-Bt-Ilm
SPP-22037	31° 39′ 34′′	67° 53′ 04′′	Flores	Metaconglomerate	Qtz-Pl-Kfs-Bt-Ms-Chl-Ep
SPP-27012	31° 35′ 48′′	67° 51′ 36′′	Flores	Metaconglomerate	Qtz-Pl-Kfs-Bt-Ms-Chl-Ep
SPP-6086	31° 43′ 00′′	68° 05′ 48′′	Flores	Metaconglomerate	Qtz-Pl-Kfs-Bt-Ms-Chl-Amph-Ep
PPL-15	31° 42′ 22′′	68° 05′ 43′′	Flores	Ca-pelitic schist	Grt-Hbl-Ms-Chl-Qtz-Pl-Ep
PPL-23	31° 42′ 55′′	68° 05′ 42′′	Flores	Ca-pelitic schist	Grt-Hbl-Ms-Chl-Qtz-Pl-Ep
SPP-22019	31° 40′ 32′′	67° 51′ 55′′	La Loma	Quartz schist	Qtz-Pl-Bt-Ms

Table 2. Chemical analyses. *Samples analyzed at Actlabs. The remaining samples were analyzed at the Laboratory of the Instituto de Geología y Minería, Universidad Nacional de Jujuy, Argentina. Total Fe content is expressed as Fe_2O_3.

Difunta Correa Metasedimentary Sequence											
Unit	La Loma	Flores				La Bomba					
Rock type	Quartz schist	Metaconglomerates		Ca-pelitic schists		Metasandstones			Metapelites		
Sample	SPP-22019*	SPP-22037*	SPP-27012	PPL-23*	PPL-15*	SPP-22013*	SPP-27000	SPP-27003	SPP-27001	SPP-27002	SPP-424*
(weight %)											
SiO_2	74.23	75.61	63.84	46.40	40.35	66.04	75.34	69.01	52.41	59.95	56.92
TiO_2	0.64	0.68	1.07	1.45	1.60	0.27	1.09	0.85	1.05	1.00	1.59
Al_2O_3	11.69	9.72	14.62	26.22	28.88	4.23	11.20	13.80	23.26	18.79	17.84
Fe_2O_3	3.71	3.73	7.50	9.32	11.35	1.49	5.59	5.92	9.21	11.65	11.03
MnO	0.09	0.08	0.10	0.17	0.15	0.10	0.10	0.09	0.10	0.26	0.13
MgO	1.37	1.01	2.27	2.72	3.33	0.25	1.31	1.64	2.37	1.93	0.65
CaO	2.21	3.21	1.65	1.67	0.88	13.47	1.97	1.34	1.36	1.13	3.62
Na_2O	3.32	2.55	2.87	2.21	0.95	0.67	2.72	2.35	1.27	0.65	6.64
K_2O	1.84	0.94	3.39	6.64	7.23	0.94	0.72	3.09	5.84	3.07	1.36
P_2O_5	0.15	0.15	0.17	0.15	0.26	0.03	0.09	0.10	0.40	0.11	0.25
LOI	0.77	0.70	1.40	3.03	4.81	11.60	0.37	0.87	2.47	1.03	0.02
Total	100.02	98.38	98.87	99.98	99.80	99.09	100.49	99.04	99.75	99.55	100.05
(ppm)											
Cs	1.60	1.40	-	5.00	3.00	0.60	-	-	-	-	0.20
Rb	71.00	29.00	-	219.00	171.00	34.00	75.00	-	165.00	105.00	8.70
Ba	467.00	385.00	-	1,100.00	1,200.00	148.00	602.00	-	1,199.00	688.00	690.00
Th	10.10	6.22	-	10.40	13.40	6.20	12.00	-	12.00	13.00	0.90
U	2.46	3.24	-	2.30	3.90	2.49	4.00	-	4.00	3.00	0.70
Nb	11.90	6.40	-	-	-	4.10	18.00	-	21.00	21.00	40.00
Ta	1.11	0.70	-	<0.5	<0.5	0.56	-	-	-	-	1.60
K	15,276	7,804	-	55,127	60,026	7,804	5,953	-	48,452	25,447	11,291
La	30.50	28.30	-	39.20	65.60	12.10	-	-	-	-	56.10
Ce	67.70	62.50	-	79.00	127.00	27.20	-	-	-	-	121.00
Pb	8.00	9.00	-	26.00	27.00	-	-	-	-	-	-
Pr	8.42	7.28	-	-	-	3.12	-	-	-	-	-
Sr	231.00	256.00	-	143.00	91.00	179.00	202.00	-	194.00	124.00	340.00
Nd	35.20	28.40	-	35.00	60.00	11.70	-	-	-	-	67.00
P	654.85	654.85	-	654.85	1,135.07	130.97	371.08	-	1,759.37	458.40	1,091.42
Zr	598.00	176.00	-	176.00	126.00	283.00	254.00	-	190.00	138.00	790.00
Hf	13.80	4.30	-	7.00	10.00	6.40	6.00	-	5.00	3.00	16.00
Sm	7.78	5.69	-	7.80	14.20	2.36	-	-	-	-	13.50
Eu	1.57	1.27	-	1.50	2.20	0.45	-	-	-	-	4.78
Ti	3,844	4,054	-	8,695	9,618	1,595	6,548	-	6,290	5,967	9,534
Gd	6.97	4.86	-	-	-	2.16	-	-	-	-	-
Tb	1.15	0.78	-	0.80	1.50	0.37	-	-	-	-	1.70
Dy	7.03	4.54	-	-	-	2.19	-	-	-	-	-
Y	39.00	25.00	-	40.00	60.00	13.00	50.00	-	52.00	36.00	40.00
Ho	1.44	0.93	-	-	-	0.48	-	-	-	-	-
Er	4.28	2.75	-	-	-	1.49	-	-	-	-	-
Tm	0.66	0.43	-	-	-	0.24	-	-	-	-	-
Yb	4.38	2.80	-	6.50	8.20	1.64	-	-	-	-	2.70
Lu	0.70	0.45	-	0.95	1.20	0.27	-	-	-	-	0.38
Sc	7.54	7.49	-	26.50	31.00	2.85	-	-	-	-	25.00
Co	10.80	13.20	-	30.00	35.00	2.60	57.00	-	38.00	67.00	8.00
Cr	29.70	40.40	-	162.00	132.00	12.40	152.00	-	121.00	158.00	7.00
Cu	3.00	12.00	-	3.00	5.00	3.00	-	-	-	-	-
Ni	17.00	19.00	-	66.00	80.00	3.00	95.00	-	51.00	25.00	50.00
S	0.01	0.02	-	<0.01	<0.01	0.09	0.02	-	0.02	0.08	-
Sb	0.30	0.20	-	0.70	<0.10	<0.10	-	-	-	-	-
Sn	4.00	2.00	-	-	-	2.00	-	-	-	-	-
Tl	0.48	0.19	-	-	-	0.15	-	-	-	-	-
V	56.00	78.00	-	153.00	183.00	22.00	-	-	-	-	-
W	22.00	43.00	-	<1	<1	3.00	-	-	-	-	<1
Zn	65.00	47.00	-	129.00	75.00	19.00	-	-	-	-	-
Rb/Sr	0.31	0.11	-	1.53	1.88	0.19	0.37	-	0.85	0.85	0.03

Table 3. Isotope composition of samples from the Difunta Correa metasedimentary sequence.

Sample	SPP-22013	SPP-22019	SPP-22037	SPP-6086	SPP-22007C	SPP-22007D	Bulk Earth
Rock type	Calcite-rich metasandstone	Quartz schist	Meta-conglomerate	Meta-conglomerate	Phosphatic clast	Phosphatic clast	
Unit	La Bomba	La Loma	Flores	Flores	Flores	Flores	
Rb (ppm)	34	71	29	101	10.7	22.8	-
Sr (ppm)	179	231	256	160	158	408.2	-
Rb/Sr	0.18994	0.30736	0.11328	0.63125	0.06772	0.05585	-
$^{87}Rb/^{86}Sr$	0.55042	0.89094	0.32796	1.83070	0.20170	0.16334	0.08920
$^{87}Sr/^{86}Sr$	0.72377	0.72692	0.71431	0.73221	0.72163	0.72290	0.70470
$^{87}Sr/^{86}Sr_{465}$	0.72013	0.72102	0.71213	0.72008	0.72030	0.72182	0.70411
$^{87}Sr/^{86}Sr_{600}$	0.71906	0.71930	0.71150	0.71655	0.71991	0.72150	0.70394
εSr_{600}	215	218	107	179	227	250	0
Sm (ppm)	2.36	7.78	5.69	6.65	-	-	-
Nd (ppm)	11.7	35.2	28.4	30.5	-	-	-
Sm/Nd	0.20171	0.22102	0.20035	0.21803	-	-	-
$^{147}Sm/^{144}Nd$	0.12193	0.13361	0.12111	0.13180	-	-	-
$^{143}Nd/^{144}Nd$	0.51203	0.51223	0.51223	0.51225	-	-	-
$^{143}Nd/^{144}Nd_{465}$	0.51166	0.51182	0.51186	0.51184	-	-	-
$^{143}Nd/^{144}Nd_{600}$	0.51156	0.51170	0.51176	0.51173	-	-	-
εNd_{600}	-6.04	-3.20	-2.14	-2.69	-	-	-
TDM	1.64	1.53	1.33	1.47	-	-	-

schists) show similar values compared to the Ca-pelitic schist, whereas quartz schists (La Loma U.), metaconglomerates (Flores U.) and metasandstones (La Bomba U.) exhibit higher concentrations of SiO_2 (63.8–75.6 %) and the lowest contents of Al_2O_3 and K_2O (4.2–14.6 % and 0.7–3.4 % respectively; Table 2).

Geochemical variations among samples (Figure 12) reflect changes in their mineralogical composition. Modal variations of phyllosilicates (pelitic component) relative to quartz-feldspar (psammitic component) are supported by: 1) negative correlations of SiO_2 against TiO_2 ($R^2 = 0.66$; $p < 0.01$), Al_2O_3 ($R^2 = 0.98$; $p < 0.001$), Fe_2O_3 ($R^2 = 0.71$; $p = < 0.01$), MgO ($R^2 = 0.58$; $p < 0.05$), and K_2O ($R^2 = 0.77$; $p < 0.001$; Figure 12a-12e) and 2) positive correlations of TiO_2 against Fe_2O_3 ($R^2 = 0.62$; $p < 0.01$), Al_2O_3 ($R^2 = 0.56$; $p < 0.05$), and K_2O ($R^2 = 0.65$; $p < 0.01$), and of Al_2O_3 with K_2O ($R^2 = 0.85$; $p < 0.001$; Figure 13). No clear patterns between CaO, Na_2O, MnO and P_2O_5 are recognized probably because they are mobile elements (Figure 12f-12i).

Relationships between major and trace elements are shown in Figure 14. The effect of the pelitic component is reflected by a positive correlation between K_2O against Ba ($R^2 = 0.90$; $p < 0.001$) and Rb ($R^2 = 0.92$; $p < 0.001$) (Figure 14a and 14b). The highest concentrations of Zr and SiO_2 are found in metasandstones (La Bomba U.), quartz schist (La Loma U.) and metaconglomerates (Flores U.).

The REE concentration of metasedimentary rocks is strongly influenced by the grain size and mineral composition. In this sense, Cullers *et al.* (1987) found that the REE concentration is about 20 % higher in shales than in sandstones. Heavy minerals, such as zircon and garnet, contribute significantly to the increase in the heavy rare earth element (HREE) content (Morton, 1991). The chondrite-normalized (Sun and McDonough, 1989) REE diagram of the DCMS samples is shown in Figure 15. The model average composition of PCS (Proterozoic Cratonic Sandstones; Condie, 1993) and PAAS (Post-Archean Australian Shales; Taylor and McLennan, 1985) are included for comparison. The REE content in metapelites from La Bomba unit and Ca-pelitic schist from the Flores unit ranges between 170.7 and 279.9 ppm, slightly enriched with respect to PAAS. Metasandstones (La Bomba U.), metaconglomerates (Flores U.) and quartz schist (La Loma U.) show higher REE values (65.7–177.7 ppm) than PCS. All samples are characterized by a light rare earth elements (LREE) enrichment ($La_N/Eu_N = 2.87–7.30$), and a flat array (except the sample SPP-424) to the HREE ($Tb_N/Lu_N = 0.57–1.17$). In general, all samples of the DCMS exhibit a negative Eu anomaly ($Eu_N/Eu_N^* = 0.61–0.74$), which is inherited from the sediment source.

Table 4. Mineral chemistry of phosphate minerals as weight% (sample SPP-22007D1). Total Fe content as FeO.

Nº analysis	CaO	P_2O_5	F	FeO	MnO	Cl	Total
3	54.53	42.31	2.21	0.06	0.07	0.02	99.12
4	54.92	41.99	1.97	0.05	0.05	0.01	98.99
5	54.36	41.22	2.13	0.14	0.04	0.01	97.90
6	55.33	41.24	2.47	0.11	0.04	0.01	99.20
mean	54.79	41.69	2.20	0.09	0.05	0.01	98.82

Sr-Nd isotope composition of detrital rocks

The Sr-isotope composition of four siliciclastic samples is shown in Table 3. Siliclastic rocks yielded $^{87}Sr/^{86}Sr$ ratios recalculated to the time of sedimentation (*ca.* 600 Ma) between 0.71150 and 0.71930. The corresponding εSr_{600} values range from 107 to 218, *i.e.,* well above Bulk Earth.

The $^{143}Nd/^{144}Nd_{600}$ values of the four detrital rocks range from 0.51156 to 0.51176. The εNd_{600} values range from -6.04 to -2.14 and Nd depleted mantle model ages (T_{DM}) are between 1.33 and 1.64 Ga.

Phosphatic clasts

Four grains of phosphate minerals were analyzed in one phosphatic clast from metaconglomerates of the Flores unit (Table 4). The composition (weight %) is very homogenous with 1.97 to 2.47 wt % F and minor contents of FeO, MnO and Cl. They are classified as apatite-(CaF), *i.e.,* fluor-apatite (Pasero *et al.,* 2010). The $^{87}Sr/^{86}Sr$ ratio measured in two phosphatic clasts yielded values of 0.72163 and 0.72290 (Table 3).

DISCUSSION

Protoliths and sedimentary setting of the DCMS

Metamorphism is considered essentially an isochemical process, with restricted mobility of non-volatile elements (Fettes and Desmons, 2007; Vernon and Clarke, 2011). Hence, ratios between some major and trace elements and the REE contents in meta-detrital rocks should reflect the mineralogical composition of protoliths, sediment maturity, and possible source areas. High Field Strength (HFS) elements (*e.g.,* La, Th, Zr, Hf, Sc and Ti) can be used to infer the source area composition and the tectonic setting because they are immobile elements, and ratios between them do not significantly change during diagenesis and metamorphism (Bhatia and Crook, 1986). Elements like Th and La are useful for identifying igneous felsic sources, whereas Zr and La concentrations reflect the degree of either crustal recycling or input from siliceous sources. Sc and Ti are related to mafic sources (Bhatia and Crook, 1986).

Source areas composition and tectonic setting were estimated here using the plots proposed by Roser and Korsch (1988; Figure 16a and 16b), Floyd and Leveridge (1987; Figure 16c) and Bhatia and Crook (1986; Figure 16d-16f). The DCMS samples suggest predominantly felsic-to-intermediate source areas with scarce influence of mafic rocks. Furthermore, most data point to continental and passive margin sedimentation (Figure 16d-16f). As it was pointed out above, these tectonic setting discrimination diagrams have to be used with caution because they often show erroneous results (Armstrong-Altrin and Verma 2005; Verdecchia and Baldo, 2010). Thus, we use here these diagrams to better constrain the tectonic setting of the basin but regional geological evidence is also considered. Marbles with sea-water Sr-isotope composition (*i.e.,* Vallecito unit; Galindo *et al.,* 2004), phosphatic clasts in the Flores unit and the lack of contemporaneous arc related igneous rocks further support passive margin sedimentation. A similar interpretation was proposed by Rapela *et al.* (2015) based on detrital zircon geochronology of the DCMS.

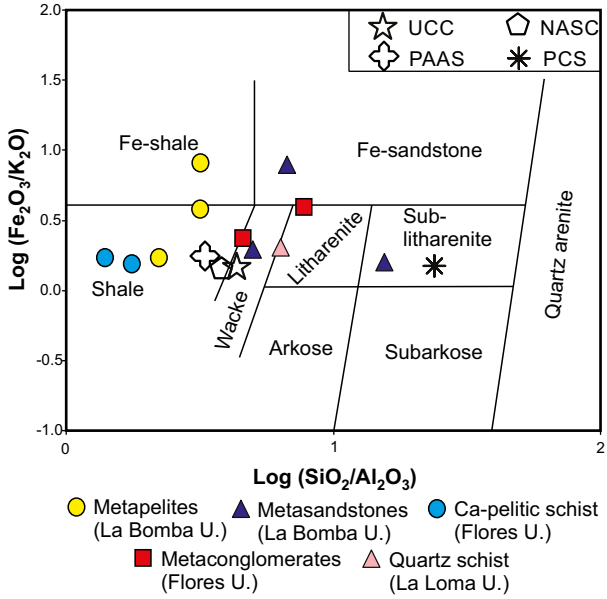

Figure 11. Herron (1988) classification diagram of sedimentary rocks. UCC: Upper Continental Crust (McLennan, 2001); PAAS: Post-Archean Australian Shales (Taylor and McLennan, 1985); NASC: North American Shale Composite (Gromet *et al.,* 1984); PCS: Proterozoic Cratonic Sandstones (Condie, 1993).

Significance of Sr- and Nd-isotope composition of detrital rocks

As siliciclastic rocks are composed of detrital minerals and clasts, the whole-rock isotope signature may be a mixture of components coming from different sources with different isotope compositions and different ages. The variations in the $^{87}Sr/^{86}Sr_{600}$ ratios (0.71150–0.71930) and the εSr_{600} values (107–218) of the four siliciclastic samples (Table 3) can thus be attributed to a mixture of components from different sources. The high values of εSr_{600} suggest that the siliciclastic rocks resulted from the erosion of an evolved continental crust.

Nd-isotope composition as shown by the εNd_{600} values between -2.14 and -6.04 (Table 3) also suggests contribution mainly from an evolved continental source. Nd model ages (T_{DM}) between 1.3 and 1.6 Ga further imply that the continental source was chiefly Mesoproterozoic (and probably older). Metasedimentary rocks of the Precambrian basement in the WSP (Sierra de Pie de Palo, Maz, Espinal and Umango; Figure 1a), yield Nd T_{DM} ages between 1.2 and 2.7 Ga (Figure 17; Varela *et al.,* 2003; Porcher *et al.,* 2004; Casquet *et al.,* 2008). A first group of ages (between 1.7 and 2.7 Ga) are restricted to the Maz suspect terrane in the sierras de Maz and Espinal. The latter consists of a strip of metasedimentary rocks that hosts a middle Mesoproterozoic juvenile magmatic arc and late Mesoproterozoic massif-type anorthosites with U-Pb ages between *ca.* 1.3 and 1.07 Ga (Casquet *et al.,* 2005a, b; Rapela *et al.,* 2010). On the other hand, the second group of model ages (between 1.2 and 1.6 Ga) involve a significant Nd contribution from Mesoproterozoic igneous sources and from reworking of older sedimentary and/or igneous rocks. This group corresponds not only to the DCMS of the SPP but also to metasedimentary successions with extensive marble beds in the sierras de Maz and Espinal (Casquet *et al.,* 2008) and in the westernmost Sierra de Umango, probably equivalent to the DCMS, where a Mesoproterozoic basement has also been recognized (Varela *et al.,* 2011). In all cases, as in the SPP, the original relationships between the second group of metasedimentary rocks and the Mesoproterozoic basement are overprinted by ductile shearing and/or faulting. However, the argument that the metasedimentary successions of the second group of Nd model ages were laid down on the Mesoproterozoic basement that outcrops in the WSP seems well-founded as they are commonly juxtaposed. Isotope geochemistry and detrital zircon evidence (*i.e.* the abundance of Mesoproterozoic ages) in this second group of metasedimentary rocks (Casquet *et al.,* 2008; Rapela *et al.,* 2015) further strengthen this interpretation.

We thus infer that the main source of the DCMS was the Mesoproterozoic basement that crops out in the sierras de Maz, Espinal, Umango and in the Central Complex of SPP. This basement underlaid the DCMS at the time of sedimentation. Moreover, rocks with Nd isotope composition similar to the DCMS are also exposed in southeastern Laurentia (present position) in the Grenville and Granite-Rhyolite provinces (Figures 17 and 18). These foreign sources have also been invoked -particularly the second- to explain some peculiarities of the detrital zircon patterns such as a population of grains between 1.3 and 1.5 Ga with no likely sources in the WSP Mesoproterozoic basement (Rapela *et al.,* 2015).

Phosphatic clasts in the Flores unit

The $^{87}Sr/^{86}Sr$ ratios in phosphorites (if not modified by later processes) should reflect the isotope composition of sea-water at the time of deposition (McArthur *et al.,* 1990; Compton *et al.,* 2002). Previous contributions (Galindo *et al.,* 2004) found $^{87}Sr/^{86}Sr$ ratios between 0.70732 and 0.70742 in marbles of the DCMS which point to an early Ediacaran depositional age according to the Sr-isotope composition of sea-water in the middle to late Neoproterozoic (Halverson and Shields, 2011). The difference between the $^{87}Sr/^{86}Sr$ ratios of the DCMS marbles and those of phosphatic clasts (0.71991 and 0.72150 at 600 Ma) sug-

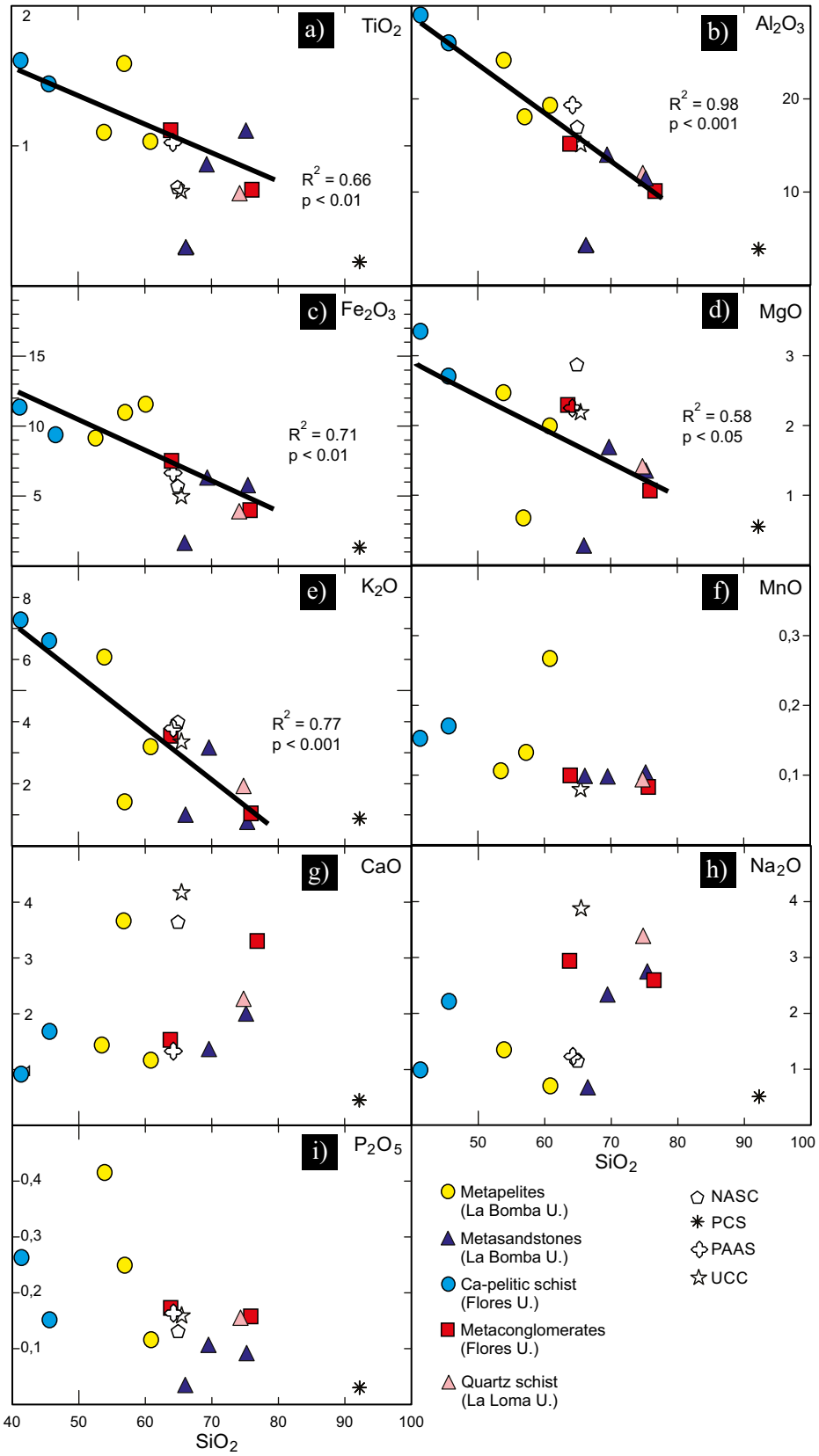

Figure 12. Chemical variation plots of metasedimentary rocks from the Difunta Correa metasedimentary sequence. Samples SPP-22013 and SPP-424 are not shown in the CaO and Na_2O plots (respectively) because contents of these components are off-scale. Values in weight percent. Sample SPP-22013 was not considered in correlation coefficients due to their carbonaceous cement.

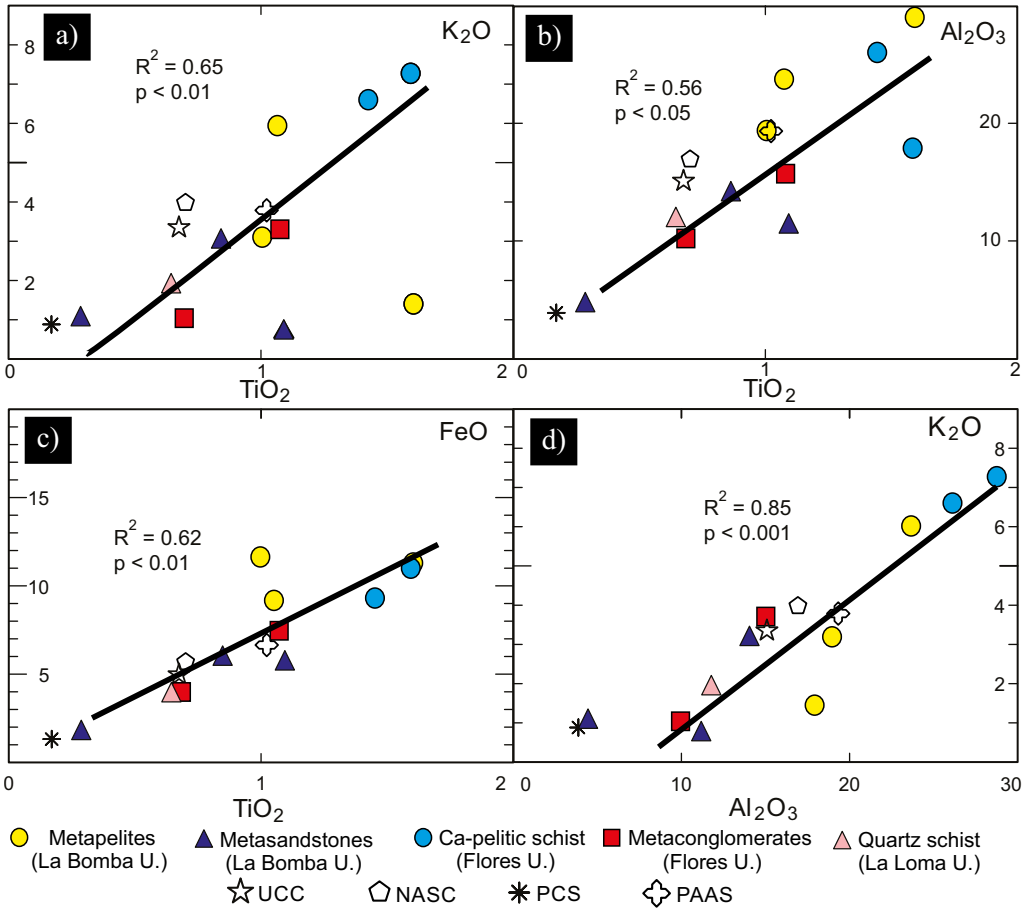

Figure 13. Variation plots of major elements against TiO_2 and Al_2O_3. Values in weight percent. a) Sample PPL-424 was not considered in correlation coefficients. b) - d) Sample SPP-22013 was not considered in correlation coefficients due to their carbonaceous cement.

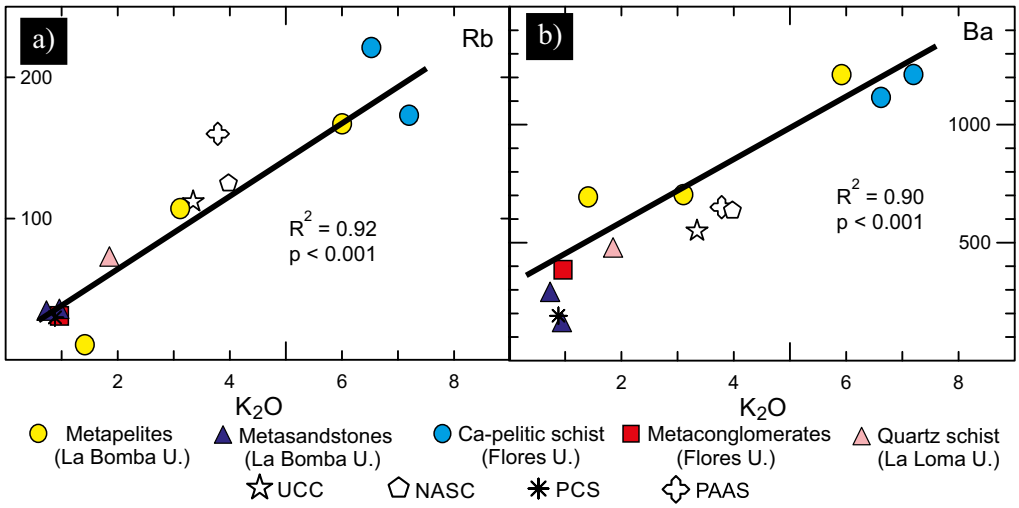

Figure 14. Variation plots of Rb and Ba of metasedimentary rocks from the Difunta Correa metasedimentary sequence. Values in weight percent for major elements and ppm for trace elements. Sample SPP-22013 was not considered in correlation coefficients due to their carbonaceous cement.

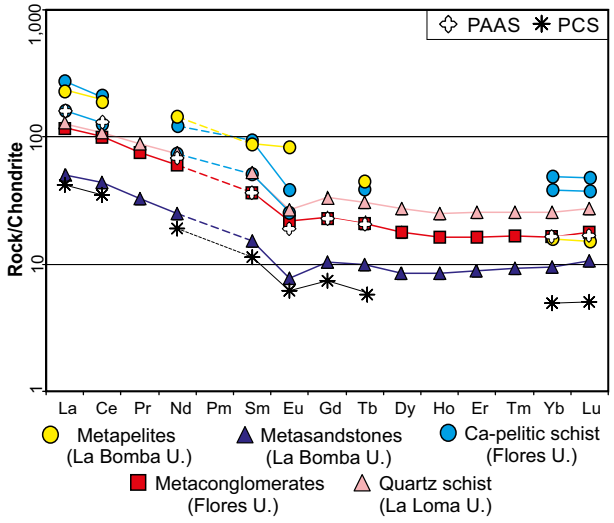

Figure 15. Chondrite-normalized (Sun and McDonough, 1989) REE diagram of samples from the Difunta Correa metasedimentary sequence.

gests that clast-forming phosphate was isotopically modified. In fact, radiogenic Sr is lost from clastic K-phyllosicates (muscovite and K-clays minerals) during heating and can be taken up by apatite (Wasserburg *et al.,* 1964; Baadsgaard and Van Breemen, 1970), raising the $^{87}Sr/^{86}Sr$ ratios of phosphatic rocks. Moreover, the $^{87}Sr/^{86}Sr$ ratio of phosphate clasts at the age of Famatinian metamorphism (*ca.* 465 Ma; Casquet *et al.,* 2001) is remarkably similar (0.72030 and 0.72182) to three of the siliciclastic samples from the DCMS (0.72009–0.72102; Table 3). Thus, phosphatic clasts probably underwent isotope exchange with the host siliciclastic matrix during metamorphism, favored by the relatively small size of the clasts and the strong compositional disequilibrium with the matrix. This exchange between phosphatic clasts and matrix can explain the outer zone (apatite rich) shown around some clasts (Figure 6a).

The phosphatic clasts were derived from the erosion of older phosphorite bodies. Phosphogenic events in the Neoproterozoic were episodic and of global extent (Cook and McElhinny, 1979; Bentor, 1980; Sheldon, 1980, 1981; Cook and Shergold, 2005; Xiao *et al.,* 2012) and time-related with glaciations (Cook and McElhinny, 1979; Sheldon, 1980, 1981; Cook, 1992; Bertrand-Sarfati *et al.,* 1997; Cook

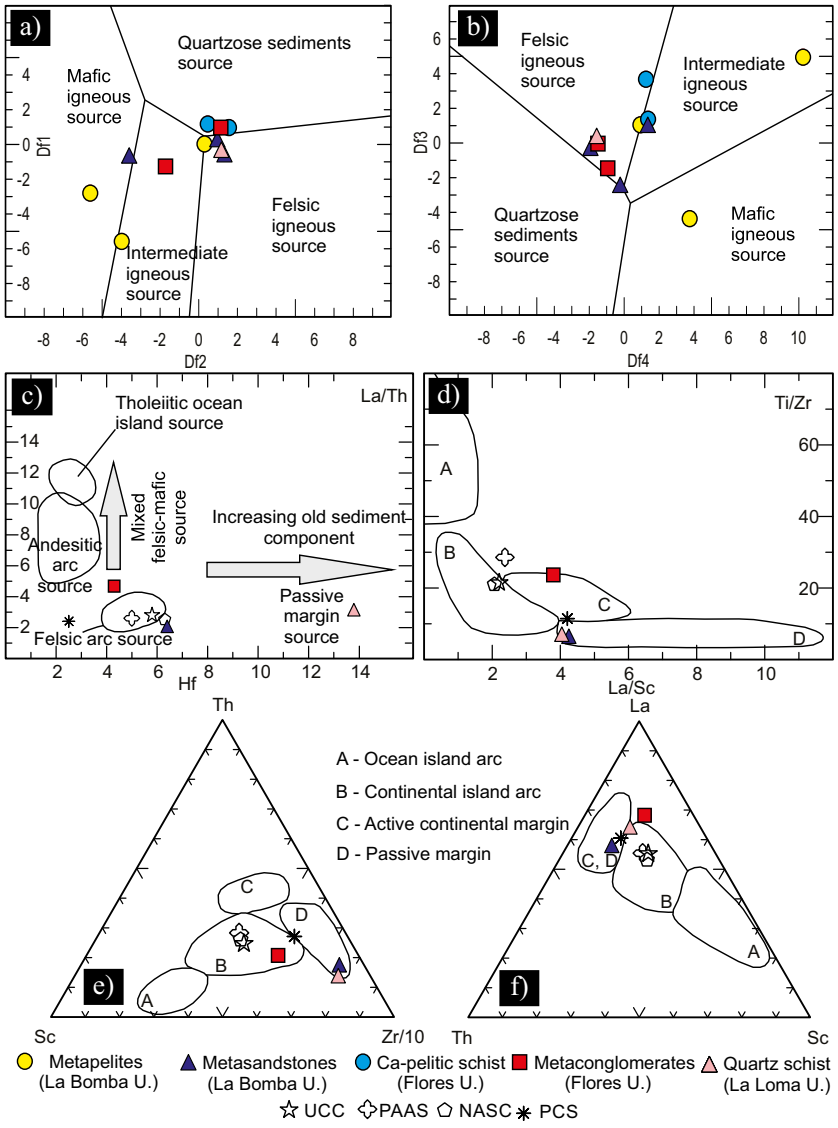

Figure 16. Source areas and tectonic setting diagrams. a) and b) Roser and Korsch, (1988). Discriminant function (Df) calculated as: Df1 = 56.500 TiO_2/Al_2O_3 - 10.879 Fe_2O_3/Al_2O_3 + 30.875 MgO/Al_2O_3 - 5.404 Na_2O/Al_2O_3 + 11.112 K_2O/Al_2O_3 - 3.89; Df2 = 30.638 TiO_2/Al_2O_3 - 12.541 Fe_2O_3/Al_2O_3 + 7.329 MgO/Al_2O_3 + 12.031 Na_2O/Al_2O_3 + 35.402 K_2O/Al_2O_3 - 6.382; Df3 = 0.445 TiO_2 + 0.070 Al_2O_3 - 0.250 Fe_2O_3 - 1.142 MgO + 0.438 CaO + 1.475 Na_2O + 1.426 K_2O - 6.861; Df4 = -1.773 TiO_2 + 0.607 Al_2O_3 + 0.760 Fe_2O_3 - 1.500 MgO + 0.616 CaO + 0.509 Na_2O - 1.224 K_2O -9.090. In all discriminant functions Fe_2O_3 represents total Fe content. c) Floyd and Leveridge (1987). d) - f) Bhatia and Crook (1986).

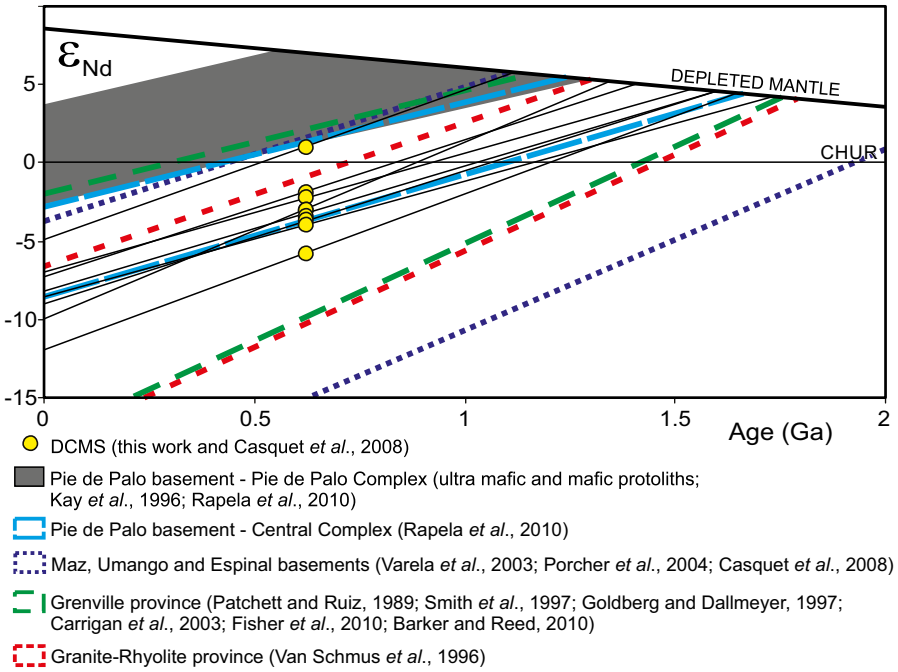

Figure 17. Comparison of isotope data of the Difunta Correa metasedimentary sequence (DCMS), with the probable source areas.

and Shergold, 2005). Considering that the marbles of the Vallecito unit probably formed in the early Ediacaran (*ca.* 600; Murra *et al.,* 2014; Rapela *et al.,* 2015) and that the Flores unit is stratigraphically older, we can speculate that phosphorite protoliths of the phosphatic clast probably formed near the Cryogenian-Ediacaran boundary, after the Marinoan (*ca.* 630 Ma) glaciation. However, unequivocal evidence for glaciogenic rocks in the lower DCMS has not been found yet.

The Neoproterozoic Sierras Bayas Group in the Tandilia System that overlies the Río de la Plata craton in southeastern Buenos Aires province, contains limestones with Sr-isotope composition similar to the DCMS marbles (Gómez Peral *et al.,* 2007, 2014). Two phosphogenic events were recognized in the Tandilia System (Gómez Peral *et al.,* 2014) that could thus be correlated with the protolith of the DCMS phosphatic clasts. In fact, Gaucher *et al.* (2008) suggested that the WSP was attached to the Río de la Plata craton in the Neoproterozoic and constituted a source area for the Sierras Bayas Group. However, detrital zircon age patterns from the Sierras Bayas Group (Rapela *et al.,* 2007; Gaucher *et al.,* 2008; Cingolani *et al.,* 2010) are significantly different from those of the DCMS (Rapela *et al.,* 2005; 2015). Although the Sierras Bayas Group contains late Mesoproterozoic zircons (between *ca.* 1.0 and 1.2 Ga) the dominant peaks are *ca.* 1.5 Ga, 2.0–2.2 Ga, 2.45 Ga and 2.7–2.8 Ga. However, the latter are absent or poorly represented in the DCMS. Therefore, detrital zircon data suggests that the source areas of the DCMS and the Sierras Bayas Group were different.

A paleogeographic scenario

Elemental and isotope geochemistry, as well as geological evidence suggest that the Ediacaran DCMS was probably deposited on a felsic to intermediate continental basement at a continental passive margin. The main source of the DCMS was probably the Mesoproterozoic basement that crops out in the sierras de Maz, Espinal, Umango and in the Central Complex of SPP. This basement underlaid the DCMS at the time of sedimentation. Furthermore, rocks with Nd isotope composition similar to the DCMS are also exposed in southeastern Laurentia (present position), in the Grenville and Granite-Rhyolite provinces (Figures 17 and 18). These Laurentian sources have also been invoked –particularly the second- to explain the detrital zircon patterns with no likely sources in the WSP Mesoproterozoic basement (Rapela *et al.,* 2015).

The relationships between the DCMS and the mafic-ultramafic Pie de Palo Complex remain unknown because both are separated by the Duraznos thrust that underwent displacement during the Ordovician and the Silurian (Mulcahy *et al.*, 2011) (Figure 2). Moreover, the juvenile Pie de Palo Complex - and the Caucete Group - probably was part of the Precordillera terrane, exotic or simply allocthonous, which reached a position close to the present in the Middle to late Ordovician (Ramos *et al.* 1998; Thomas and Astini, 2003; Astini and Dávila, 2004).

Our data are compatible with the idea that the WSP basement was part of the MARA continental block (Casquet *et al.,* 2012). According to this hypothesis the southeastern passive margin of Laurentia in the Neoproterozoic was not the Appalachian margin but the eastern (present position) MARA margin, where the original sediments of the DCMS were laid down in the Puncoviscana/Clymene Ocean (Figure 18).

CONCLUSIONS

Metasedimentary rocks from the DCMS were classified as shales, Fe-shale and immature sandstones (wacke, sub-litharenite, litharenite and Fe-sandstone) based on chemical parameters. Modal variations of phyllosilicates (mainly pelitic component) and quartz-feldspar (psammitic component) are supported by negative correlations of TiO_2, Al_2O_3, Fe_2O_3, MgO and K_2O with SiO_2 and positive correlations of Fe_2O_3, Al_2O_3, and K_2O against TiO_2, and of Al_2O_3 with K_2O. Almost all samples exhibit a negative Eu anomaly (Eu_N/Eu_N^* = 0.61–0.74), which indicates a typical continental crust composition.

At least part of the DCMS is of marine origin and the detrital sediments came from a felsic to intermediate continental source and were deposited on the continental passive margin of the MARA block

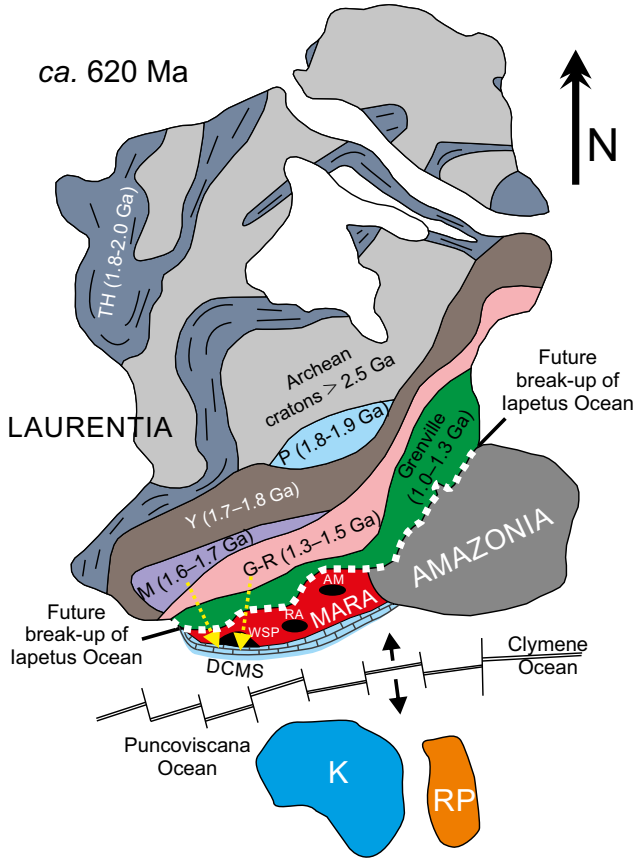

Figure 18. Paleogeographical reconstruction of Laurentia, Amazonia, Río de la Plata (RP) and Kalahari (K) showing the guessed position of MARA (acronym of Maz, Arequipa, Rio Apa) craton at *ca.* 620 Ma. Ages of Laurentian Precambrian orogenic belts and cratons according to Goodge *et al.* (2004) and Tohver *et al.* (2004) (Laurentia in its present position). Outcrops of basement with Mesoproterozoic ages in MARA have been included: AM, Arequipa Massif (Peru); RA, Rio Apa (Brazil, Paraguay); WSP, Western Sierras Pampeanas (Argentina). Laurentia: TH, Trans-Hudson and related mobile belts; P, Penokean orogen; Y, Yavapai orogen; M, Mazatzal orogen; G-R, Granite-Rhyolite province. Arrows show the hypothetical direction of sediment transport from the probable source areas of the Difunta Correa metasedimentary sequence (DCMS).

in the Puncoviscana/Clymene Ocean. This source probably laid in the Mesoproterozoic basement of the WSP and in the Grenville and Granite-Rhyolite provinces of southeastern Laurentia.

The phosphatic clasts from the Flores unit probably correspond to reworking of phosphorites formed after one of the worldwide Neoproterozoic glaciations. Because the age of the lower tract of the DCMS can be constrained to be younger than *ca.* 630 Ma we suggest that this glaciation was the Marinoan, although glaciogenic sediments have not been firmly recognized yet in this part of the Sierras Pampeanas.

ACKNOWLEDGEMENTS

This paper is part of the first author´s doctoral thesis. This research was funded by the Universidad Nacional de Córdoba, Argentina (SECyT-2014/2015) and by Spanish grants CGL2009-07984 and GR58/08 UCM-Santander. We are grateful to the Editor Dr. Luigi Solari, to Roelant van der Lelij and one anonymous reviewer for corrections and suggestions that improved this manuscript. We acknowledge Dr. U. Zimmermann (University of Stavanger, Norway) and Dr. E. Le Pera (Universitá della Calabria, Italy) for their helpful comments on an earlier draft of the paper. Dr. R. J. Pankhurst improved the english editing of the paper. Moreover we are indebted to all the members of the PAMPRE research group.

REFERENCES

Abràmoff, M.D., Magalhães, P.J., Ram, S.J., 2004, Image Processing with ImageJ: Biophotonics International, 11, 36-42.

Abbruzzi, J.M., Kay, S.M., Bickford, M.E., 1993, Implications for the nature of the Precordilleran basement from the geochemistry and age of Precambrian xenoliths in Miocene volcanic rocks, San Juan province, *in* 12º Congreso Geológico Argentino and 2º Congreso Exploración de Hidrocarburos: Mendoza, Argentina, Actas, 3, 331-339.

Allègre, C.J., Hart, S.R., Minster, J.F., 1983, Chemical structure and evolution of the mantle and continents determined by inversion of Nd and Sr isotopic data, I. Theoretical models: Earth and Planetary Science Letters, 66, 177-190. doi:10.1016/0012-821X(83)90135-8.

Armstrong-Altrin, J., Verma, S., 2005, Critical evaluation of six tectonic setting discrimination diagrams using geochemical data of Neogene sediments from known tectonic settings: Sedimentary Geology, 177, 115-129. doi:10.1016/j.sedgeo.2005.02.004.

Arribas, J., Critelli, S., Johnsson, M.J., 2007, Sedimentary Provenance and Petrogenesis: Perspectives from Petrography and Geochemistry: Boulder, Colorado, Geological Society of America Special Paper, 420, 396 p.

Astini, R.A., Dávila, F.M., 2004, Ordovician back-arc foreland and Ocloyic thrust belt development on the western Gondwana margin as a response to Precordillera terrane accretion: Tectonics, 23, 1-19. doi:10.1029/2003TC001620.

Baadsgaard, H., Van Breemen, O., 1970, Thermally induced migration of Rb and Sr in an adamellite: Eclogae Geologicae Helvetiae, 63, 31-44. doi:org/10.5169/seals-163812.

Baldo, E.G., Casquet, C., Galindo, C., 1998, Datos preliminares sobre el

metamorfismo de la Sierra de Pie de Palo, Sierras Pampeanas Occidentales (Argentina): Geogaceta, 24, 39-42

Baldo, E.G., Casquet, C., Pankhurst, R.J., Galindo, C., Rapela, C.W., Fanning, C.M., Dahlquist, J.A., Murra, J., 2006, Neoproterozoic A-type magmatism in the Western Sierras Pampeanas (Argentina): evidence for Rodinia break-up along a proto-Iapetus rift?: Terra Nova, 18, 388-394. doi: 10.1111/j.1365-3121.2006.00703.x.

Baldo, E.G., Dahlquist, J.A., Casquet, C., Rapela, C.W., Pankhurst, R.J., Galindo, C., Fanning, C.M., Ramacciotti, C., 2012, Ordovician peraluminous granites in the Sierra de Pie de Palo, Western Sierras Pampeanas of Argentina: Geotectonic Implications, *in* VIII Congreso Geológico de España: Geo-Temas 13, 569.

Barker, D.S., Reed, R.M., 2010, Proterozoic granites of the Llano Uplift, Texas: A collision-related suite containing rapakivi and topaz granites: Geological Society of America Bulletin, 122(1-2), 253-264.

Bentor, Y.K., 1980, Phosphorites -the unsolved problems, *in* Bentor, Y.K. (ed.), Marine Phosphorites-Geochemistry, Occurrence, Genesis: Society of Economic Paleontologists and Mineralogists Special Publication, 29, 3-18.

Bertrand-Sarfati, J., Flicoteaux, R., Moussine-Pouchkine, A., Ahmed, A.A.K., 1997, Lower Cambrian apatitic stromatolites and phosphorites related to the glacio-eustatic cratonic rebound (Sahara, Algeria): Journal of Sedimentary Research, 67, 957-974. doi:10.1306/D426868A-2B26-11D7-8648000102C1865D.

Bhatia, M., Crook, K., 1986, Trace element characteristics of graywackes and tectonic setting discrimination of sedimentary basins: Contributions to Mineralogy and Petrology, 92, 181-193. doi:10.1007/BF00375292.

Borrello, A.V., 1969, Los geosinclinales de la Argentina: Buenos Aires, Dirección Nacional de Geología y Minería, Anales, 14, 1-136.

Carrigan, C.W., Miller, C.F., Fullagar, P.D., Bream, B.R., Hatcher, R.D., Jr., Coath, C.D., 2003, Ion microprobe age and geochemistry of southern appalachian basement, with implications for Proterozoic and Paleozoic reconstructions: Precambrian Research, 120, 1-36.

Casquet, C., Baldo, E.G., Pankhurst, R.J., Rapela, C.W., Galindo, C., Fanning, C.M., Saavedra, J., 2001, Involvement of the Argentine Precordillera terrane in the Famatinian mobile belt: U-Pb SHRIMP and metamorphic evidence from the sierra de Pie de Palo: Geology, 29, 703-706. doi:10.1130/0091-7613(2001)029<0703:IOTAPT>2.0.CO;2.

Casquet, C., Rapela, C.W., Pankhurst, R.J., Galindo, C., Dahlquist, J., Baldo, E.G., Saavedra, J., González-Casado, J.M., Fanning, C.M., 2005a, Grenvillian massif-type anorthosites in the Sierras Pampeanas: Journal of the Geological Society, 162, 9-12. doi:10.1144/0016-764904-100.

Casquet, C., Pankhurst, R.J., Rapela, C.W., Fannning, C.M., Galindo, C., Baldo, E., González-Casado, J.M., Dahlquist, J., Saavedra, J., 2005b, The Maz suspect terrane: a new Proterozoic domain in the Western Sierras Pampeanas, *in* Pankhurst, R.J., Veiga, G.D. (eds.), Gondwana 12th Conference, Geological and Biological Heritage of Gondwana: Mendoza, Argentina, Academia Nacional de Ciencias, Abstract, 92.

Casquet, C., Pankhurst, R.J., Rapela, C., Galindo, C., Fanning, C.M., Chiaradia, M., Baldo, E., González-Casado, J.M., Dahlquist, J.A., 2008, The Mesoproterozoic Maz terrane in the Western Sierras Pampeanas, Argentina–Antofalla block of southern Peru? Implications for Western Gondwana margin evolution: Gondwana Research, 13, 163-175. doi:10.1016/j.gr.2007.04.005.

Casquet, C., Rapela, C.W., Pankhurst, R.J., Baldo, E.G., Galindo, C., Fanning, C.M., Dahlquist, J.A., Saavedra, J., 2012, A history of Proterozoic terranes in southern South America: From Rodinia to Gondwana: Geoscience Frontiers, 3, 137-145. doi:10.1016/j.gsf.2011.11.004.

Cingolani, C.A., Uriz, N.J., Chemale Jr, F., 2010, New U-Pb detrital zircon data from the Tandilia Neoproterozoic units, *in* Proceedings of 7th South American symposium on isotope geology: Brasilia, Actas, 1-3,

Compton, J.S., Mulabisana, J., McMillan, I.K., 2002, Origin and age of phosphorite from Last Glacial Maximum to Holocene transgressive succession off the Orange River, South Africa: Marine Geology, 186, 243-261. doi:10.1016/S0025-3227(02)00211-6.

Condie, K., 1993, Chemical composition and evolution of the upper continental crust: Contrasting results from surface samples and shales: Chemical Geology, 104, 1-37. doi:10.1016/0009-2541(93)90140-E.

Cook, P., 1992, Phosphogenesis around the Proterozoic–Phanerozoic transition: Journal of the Geological Society, 149, 615-620. doi:10.1144/gsjgs.149.4.0615.

Cook, P.J., McElhinny, M.W., 1979, A re-evaluation of the spatial and temporal distribution of sedimentary phosphate deposits in the light of plate tectonics: Economic Geology, 74, 315-330. doi:10.2113/gsecongeo.74.2.315.

Cook, P.J., Shergold, J.H., 2005, Phosphate Deposits of the World. Proterozoic and Cambrian Phosphorites: Cambridge, Cambridge University Press, 1, 386 pp.

Cullers, R.L., Barrett, T., Carlson, R., Robinson, B., 1987, Rare-Earth element and mineralogic changes in Holocene soil and stream sediment: a case study in the wet mountains region, Colorado, USA: Chemical Geology, 63, 275-297. doi:10.1016/0009-2541(87)90167-7.

DePaolo, D.J., 1988, Neodymium isotopes geochemistry: An introduction: New York, Springer Verlag, 187 pp.

Dickinson, W.R., Suczek, C.A., 1979, Plate tectonics and sandstone composition: American Association of Petroleum Geologists Bulletin, 63, 2164-2182.

Faure, G., 2001, Origin of Igneous Rocks; The Isotopic Evidence: Heidelberg, Springer-Verlag, 589 pp.

Fettes, D., Desmons J., 2007, Metamorphic Rocks: A Classification and Glossary of Terms: Cambridge, Cambridge University Press, 258 pp.

Fisher, C.M., Loewy, S.L., Miller, C.F., Berquist, P., Van Schmus, W.R., Hatcher, R.D., Jr., Wooden, J.L., Fullagar, P.D., 2010, Whole-rock Pb and Sm-Nd isotopic constraints on the growth of southeastern Laurentia during Grenvillian orogenesis: Geological Society of America Bulletin, 122(9-10), 1646-1659.

Floyd, P., Leveridge, B., 1987, Tectonic environment of the Devonian Gramscatho basin, south Cornwall: framework mode and geochemical evidence from turbiditic sandstones: Journal of the Geological Society, 144, 531-542. doi:10.1144/gsjgs.144.4.0531.

Galindo, C., Casquet, C., Rapela, C.W., Pankhurst, R.J., Baldo, E., Saavedra, J., 2004, Sr, C, and O isotope geochemistry and stratigraphy of Precambrian and lower Paleozoic carbonate sequences from the western Sierras Pampeanas of Argentina: tectonic implications: Precambrian Research, 131, 55-71. doi:10.1016/j.precamres.2003.12.007.

Garber, J., Roeske, S.M., Warren, J., Mulcahy, S.R., McClelland, W.C., Austin, L., Renne, P.R., Vujovich, G.I., 2014, Crustal shortening, exhumation, and strain localization in a collisonal orogen: the Bajo Pequeno shear zone, Sierra de Pie de Palo, Argentina: Tectonics, 33, 1277-1303. doi:10.1002/2013TC003477.

Gaucher, C., Finney, S.C., Poiré, D.G., Valencia, V.A., Grove, M., Blanco, G., Pamoukaghlián, K., Gómez-Peral, L., 2008, Detrital zircon ages of Neoproterozoic sedimentary successions in Uruguay and Argentina: insights into the geological evolution of the Río de la Plata Craton: Precambrian Research, 167, 150-170. doi:10.1016/j.precamres.2008.07.006.

Goldberg, S.A., Dallmeyer, R.D., 1997, Chronology of Paleozoic metamorphism and deformation in the Blue Ridge thrust complex, North Carolina and Tennessee: American Journal of Science, 297, 488-526.

Goldstein, S.J., O'Nions, R.K., Hamilton, P.J., 1984, A Sm-Nd isotopic study of atmospheric dusts and particulates from major river systems: Earth and Planetary Science Letters, 70, 221-236. doi:10.1016/0012-821X(84)90007-4.

Gómez-Peral, L.E., Poiré, D.G., Strauss, H., Zimmermann, U., 2007, Chemostratigraphy and diagenetic constraints on Neoproterozoic carbonate successions from the Sierras Bayas Group, Tandilia System, Argentina: Chemical Geology, 237, 109-128. doi:10.1016/j.chemgeo.2006.06.022.

Gómez-Peral, L.E., Kaufman, A.J., Poiré, D.G., 2014, Paleoenvironmental implications of two phosphogenic event in Neoproterozoic sedimentary successions of the Tandilia System, Argentina: Precambrian Research, 252, 88-106. doi.org/10.1016/j.precamres.2014.07.009.

Goodge, J.W., Williams, I.S., Myrow, P., 2004, Provenance of Neoproterozoic and lower Paleozoic siliciclastic rocks of the Central Ross orogeny, Antarctica: detrital record of rift-, passive and active-margin sedimentation: Geological Society of America Bulletin, 116, 1253-1279. doi: 10.1130/B25347.1.

Gromet, L.P., Dymek, R.F., Haskin, L.A., Korotev, R.L., 1984, The "North American Shale Composite": Its compilation, major and trace elements characteristics: Geochimica et Cosmochimica Acta, 48, 2469-2482. doi:10.1016/0016-7037(84)90298.

Halverson, G.P., Shields, G., 2011, Chemostratigraphy and the Neoproterozoic glaciations, *in* Arnaud, E., Halverson, G.P., Shields-Zhou, G., (eds.), The Geological Record of Neoproterozoic Glaciations: London, The Geological

Society, 51-66. doi:10.1144/M36.4.
Herron, M.M., 1988, Geochemical classification of terrigenous sands and shales from core or log data: Journal of Sedimentary Petrology, 58, 820-829. doi:10.1306/212F8E77-2B24-11D7-8648000102C1865D.
Isacks, B.L., 1988, Uplift of the Central Andean Plateau and bending of the Bolivian Orocline: Journal of Geophysical Research, 93, 3211-3231. doi:10.1029/JB093iB04p03211.
Jacobsen, S.B., Wasserburg, G.J., 1980, Sm–Nd isotopic evolution of chondrites: Earth and Planetary Science Letters, 50, 139-155. doi:10.1016/0012-821X(84)90109-2.
Johnsson, M.J., 1993, The system controlling the composition of clastic sediments, *in* Johnsson, M.J., Basu, A. (eds.), Processes Controlling the Composition of Clastic Sediments: Boulder, Colorado, Geological Society of America Special Paper, 284, 1-19.
Jordan, T.E., Allmendinger, R.W., 1986, The Sierras Pampeanas of Argentina; a modern analogue of the Rocky Mountain foreland deformation: American Journal of Science, 286, 737-764. doi:10.2475/ajs.286.10.737.
Kay, S.M., Orrell, S., Abbruzzi, J.M., 1996, Zircon and whole rock Nd-Pb isotopic evidence for a Grenville age and a Laurentian origin for the Precordillera terrane in Argentina: The Journal of Geology, 104, 637-648. doi:10.1086/629859.
Kretz, R., 1983, Symbols for rock-forming minerals: American Mineralogist, 68, 277-279.
Lugmair, G.W., Carlson R.W., 1978, The Sm–Nd history of KREEP, *in* Ninth Lunar and Planetary Science Conference, Houston: New York, Pergamon Press, Proceedings, 1, 689-704.
McArthur, J.M., Sahami, A.R., Thirlwall, M., Hamilton, P.J., Osborn, A.O., 1990, Dating phosphogenesis with strontium isotopes: Geochimica et Cosmochimica Acta, 54, 1343-1351. doi:10.1016/0016-7037(90)90159-I.
McDonough, M.R., Ramos, V.A., Isachsen, C.E., Bowring, S.A., Vujovich, G.I., 1993, Nuevas edades de circones del basamento de la sierra de Pie de Palo, Sierras Pampeanas Occidentales de San Juan: sus implicancias para los modelos del supercontinente proterozoico de Rodinia, *in* XII Congreso Geológico Argentino y II Congreso de Exploración de Hidrocarburos: Mendoza, Argentina, Academia Nacional de Ciencias, Actas, III, 340-342.
McLennan, S., 1989, Rare Earth elements in sedimentary rocks: influence of provenance and sedimentary process, *in* Lipin, B., Mckay, G. (eds), Geochemistry and mineralogy of Rare Earth elements: Mineralogical Society of America, Reviews in Mineralogy, 21, 169-200.
McLennan, S., 2001, Relationship between the trace element composition of sedimentary rocks and upper continental crust: Geochemistry, Geophysics, Geosystems, 2, 1525-2027. doi:10.1029/2000GC000109.
McLennan, S., Taylor, S., McCulloch, M., Maynard, J., 1990, Geochemical and Nd–Sr isotopic composition of deep-sea turbidites: crustal evolution and plate tectonic associations: Geochimica et Cosmochimica Acta, 54, 2015-2050. doi:10.1016/0016-7037(90)90269-Q.
McLennan, S., Bock, B., Hemmin, S., Hurowitz, J., Lev, S., McDaniel., 2003, The role of provenance and sedimentary processes in the geochemistry of sedimentary rocks, *in* Lentz, D. (ed.), Geochemistry of sediments and sedimentary rocks: evolutionary considerations to mineral deposit-forming environment: Geological Association of Canada, 4, 7-38.
Morata, D., Castro de Machuca, B., Arancibia, G., Pontoriero, S., Fanning, C.M., 2010, Peraluminous Grenvillian TTG in the sierra de Pie de Palo, Western Sierras Pampeanas, Argentina: Petrology, geochronology, geochemistry and petrogenetic implications: Precambrian Research, 177, 308-322. doi:10.1016/j.precamres.2010.01.001.
Morton, A.C., 1991, Geochemical studies of detrital heavy minerals and their application to provenance research: London, Geological Society Special Publications, 57, 31-45. doi:10.1144/GSL.SP.1991.057.01.04.
Mulcahy, S.R., Roeske, S.M., McClelland, W.C., Jourdan, F., Iriondo, A., Renne, P.R., Vervoort, J.D., Vujovich, G.I., 2011, Structural evolution of a composite middle to lower crustal section: the Sierra de Pie de Palo, northwest Argentina: Tectonics, 30, TC1005, 1-24. doi:10.1029/2009TC002656.
Murra, J., Locati, F., Galindo, C., Baldo, E., Casquet, C., Scalerandi, I., 2014, Composición isotópica (Sr- C) de los mármoles de las Sierras de Córdoba: edad de sedimentación y correlación con otros sedimentos metacarbonáticos de las Sierras Pampeanas, *in* Martino, R.D., Lira, R., Guereschi, A., Baldo, E., Franzese, J., Krohling, D., Manassero M., Ortega, G., Pinotti, L. (eds.), XIX Congreso Geológico Argentino: Córdoba Argentina, S-21, 39.
Naipauer, M., Vujovich, G.I., Cingolani, C.A., McClelland, W.C., 2010, Detrital Zircon analysis from de Neoproterozoic-Cambrian sedimentary cover (Cuyania terrane), Sierra de Pie de Palo, Argentina: Evidence of a rift and passive margin system?: Journal of South American Earth Sciences, 29, 306-326. doi:10.1016/j.jsames.2009.10.001.
Pankhurst, R.J., O'Nions, R.K., 1973, Determination of Rb/Sr and $^{87}Sr/^{86}Sr$ ratios of some standard rocks and evaluation of X-ray fluorescence spectrometry in Rb-Sr geochemistry: Chemical Geology, 12, 127-36.
Pankhurst, R.J, Rapela, C.W., 1998, The proto-Andean margin of Gondwana: an introduction, *in* Pankhurst, R.J. and Rapela, C.W., (eds.), The proto-Andean margin of Gondwana, Geological Society Special Publication, 142, 1-9. doi: 10.1144/GSL.SP.1998.142.01.01.
Pasero, M., Kampf, A.R., Ferraris, C., Pekov, I.V., Rakovan, J., White, T.J., 2010, Nomenclature of the apatite supergroup minerals: European Journal of Mineralogy, 22, 163-179. doi: 10.1127/0935-1221/2010/0022-2022.
Patchett, P.J., Ruiz, J., 1989, Nd isotopes and the origin of the Grenville-age rocks in Texas: implications for Proterozic evolution of the United States Mid-continent region: Journal of Geology, 97, 685-695.
Porcher, C.C., Fernandes, L.A.D., Vujovich, G.I., Chernicoff, C.J., 2004, Thermobarometry, Sm/Nd ages and geophysical evidence for the location of the suture zone between Cuyania and the western Proto-Andean margin of Gondwana: Gondwana Research, 7, 1057-1076. doi:10.1016/S1342-937X(05)71084-4.
Ramacciotti, C.D., Baldo, E.G., Casquet, C., Galindo, C., Verdecchia, S., 2014, Edad U-Pb SHRIMP en circones detríticos al sureste de Pie de Palo, San Juan, Argentina: evidencias de sedimentación y magmatismo paleozoico en las Sierras Pampeanas Occidentales, *en* Martino, R.D., Lira, R., Guereschi, A., Baldo, E., Franzese, J., Krohling, D., Manassero M., Ortega, G., Pinotti, L. (eds.), XIX Congreso Geológico Argentino, Córdoba, Argentina, S21-48.
Ramos, V.A., 2004, Cuyania, an exotic block to Gondwana: review of a historical success and the present problems: Gondwana Research, 7, 1009-1026. doi:10.1016/S1342-937X(05)71081-9.
Ramos, V.A., Dallmeyer, D., Vujovich, G., 1998, Time constraints on the early Palaeozoic docking of the Precordillera, central Argentina, *in* Pankhurst, R.J., and Rapela, C.W., (eds.), The Proto-Andean Margin of Gondwana, Geological Society Special Publication, 142, 143-158. doi:10.1144/GSL.SP.1998.142.01.08.
Rapela, C.W., Pankhurst, R.J., Casquet, C., Fanning, C.M., Galindo, C., Baldo, E.G., 2005, Datación U-Pb SHRIMP de circones detríticos en paranfibolitas neoproterozoicas de la secuencia Difunta Correa (Sierras Pampeanas Occidentales, Argentina): Geogaceta, 38, 227-230.
Rapela, C.W., Pankhurst, R.J., Casquet, C., Fanning, C.M., Baldo, E.G., González-Casado, J., Galindo, C., Dahlquist, J.A., 2007, The Río de la Plata Craton and the assembly of SW Gondwana: Earth-Science Reviews, 83, 49-82. doi:10.1016/j.earscirev.2007.03.004.
Rapela, C.W., Pankhurst, R.J., Casquet, C., Baldo, E.G., Galindo, C., Fanning, C.M., Dahlquist, J.A., 2010, The Western Sierras Pampeanas: protracted Grenville-age history (1330-1030 Ma) of intra-oceanic arcs, subduction and accretion at continental-edge and AMCG intraplate magmatism: Journal of South American Earth Sciences, 29, 105-127. doi:10.1016/j.jsames.2009.08.004.
Rapela, C.W., Verdecchia S.O., Casquet, C., Pankhurst, R.J., Baldo, E.G., Galindo, C., Murra, J.A., Dahlquist, J.A., Fanning, C.M., 2015, Identifying Laurentian and SW Gondwana sources in the Neoproterozoic to Early Paleozoic metasedimentary rocks of the Sierras Pampeanas: Paleogeographic and tectonic implications: Gondwana Research, 2015. doi:10.1016/j.gr.2015.02.010.
Roser, B.P., Korsch, R.J., 1988, Provenance signatures of sandstone-mudstone suites determined using discriminant function analysis of major element data: Chemical Geology, 67, 119-139. doi:10.1016/0009-2541(88)90010-1.
Selverstone, J., Spear, F.S., Franz, G., Morteani, G., 1984, High-pressure metamorphism in the SW Tauern Window, Austria: P–T paths from hornblende-kyanite-staurolite schists: Journal of Petrology, 25, 501-531. doi:10.1093/petrology/25.2.501.
Sheldon, R.P., 1980, Episodicity of phosphate deposition and deep ocean circulation – a hypothesis, *in* Bentor, Y.K. (ed.), Marine Phosphorites–Geochemistry, Occurrence, Genesis: Society of Economic Paleontologist

and Mineralogist Special Publication, 29, 239-247.
Sheldon, R.P., 1981, Ancient marine phosphates: Annual Review of Earth and Planetary Sciences, 9, 251-284.
Smith. T.E., Holm, P.E., Denisson, N.M., Harris,M.J., 1997, Crustal assimilation in the Burnt Lake metavolcanics, Grenville Province, southeastern Ontario, and its tectonic significance: Canadian Journal of Earth Science, 34(9), 1272-1285.
Steiger, R.H., Jäger, E., 1977, Subcommission of geochronology: convention on the use of decay constants in geo- and cosmochronology: Earth and Planetary Science Letters, 36, 359-362. doi:10.1016/0012-821X(77)90060-7.
Sun, S.S., McDonough, W.F., 1989, Chemical and isotopic systematics of oceanic basalts: implications for mantle composition and processes: London, Geological Society Special Publication, 42, 313-345. doi:10.1144/GSL.SP.1989.042.01.19.
Taylor, S.R., McLennan, S.M., 1985, The continental crust: its composition and evolution: Oxford, Blackwell, 312 pp.
Thomas, W.A., Astini, R.A., 2003, Ordovician accretion of the Argentine Precordillera terrane to Gondwana: A review: Journal of South American Earth Sciences, 16, 67-79. doi:10.1016/S0895-9811(03)00019-1.
Tohver, E., Bettencourt, J.S., Tosdal, R., Mezger, K., Leite, W.B., Payolla, B.L., 2004, Terrane transfer during the Grenville orogeny: Tracing the Amazonian ancestry of southern Appalachian basement through Pb and Nd isotopes: Earth and Planetary Science Letters, 228, 161-176. doi: 10.1016/j.epsl.2004.09.029
Trindade, R.I.F., D'Agrella-Filho, M.S., Epof, I., Brito Neves, B.B., 2006, Paleomagnetism of the early Cambrian Itabaiana mafic dikes, NE Brazil, and implications for the final assembly of Gondwana and its proximity to Laurentia: Earth and Planetary Science Letters, 244, 361-377. doi:10.1016/j.epsl.2005.12.039.
Van Schmus, W.R., Bickford, M.E., Turek, A., 1996, Proterozoic geology of the east-central Midcontinent basement, *in* van der Pluijm, B.A., Catacosinos, P.A., (eds.), Basement and basins of eastern North America: Geological Society of America Special Paper, 308, 7-32.
van Staal, C.R., Vujovich, G.I., Currie, K.L., 2011, An Alpine-style Ordovician collision complex in the Sierra de Pie de Palo, Argentina: Record of subduction of Cuyania beneath the Famatina arc: Journal of Structural Geology, 33, 343-361. doi:10.1016/j.jsg.2010.10.011.
Varela, R., Sato, A.M., Basei, M.A.S., Siga, O. Jr., 2003, Proterozoico medio y Paleozoico inferior de la Sierra de Umango, Antepaís Andino (29º S), Argentina, Edades U/Pb y caracterizaciones isotópicas: Revista Geológica de Chile, 30, 265-284.
Varela, R., Basei, M.A.S., González, P.D., Sato, A., Naipauer, M., Campos Neto, M., Cingolani, C.A., Meira, T., 2011, Accretion of Grenvillian terranes to the southwestern border of the Río de la Plata craton, western Argentina: International Journal of Earth Sciences, 100, 243-272. doi: 10.1007/s00531-010-0614-2.
Verdecchia, S., Baldo, E.G., 2010, Geoquímica y procedencia de los metasedimentos ordovícicos del complejo metamórfico La Cébila, Provincia de La Rioja, Argentina: Revista Mexicana de Ciencias Geológicas, 27(1), 97-111.
Vernon, R.H., Clarke, G.L., 2011, Principles of Metamorphic Petrology: Cambridge, Cambridge University Press, 478 pp.
Vujovich, G.I., 2003, Metasedimentos siliciclásticos proterozoicos en la sierra de Pie de Palo, San Juan: procedencia y ambiente tectónico: Revista de la Asociación Geológica Argentina, 58, 608-622.
Vujovich, G.I., Kay, S.M., 1998, A Laurentian? Grenville age oceanic arc/back-arc terrane in the Sierra de Pie de Palo, Western Sierras Pampeanas, Argentina, *in* Pankhrust, R.J., Rapela, C.W., (eds.), The Proto-Andean margin of Gondwana: Geological Society Special Publication, 142, 159-180. doi:10.1144/GSL.SP.1998.142.01.09.
Vujovich, G.I., van Staal, C.R., Davis, W., 2004, Age constraints on the tectonic evolution and provenance of the Pie de Palo Complex, Cuyania composite terrane, and the Famatinian Orogeny in the Sierra de Pie de Palo, San Juan, Argentina: Gondwana Research, 7, 1041-1056. doi:10.1016/S1342-937X(05)71083-2.
Wasserburg, G.J, Albeea, A.L., Lanphere, 1964, Migration of radiogenic strontium during metamorphism: Journal of Geophysical Research, 69, 4395-4401. doi:10.1029/JZ069i020p04395.
Xiao, S., McFadden, K.A., Peek, S., Kaufman, A.J., Zhou, C., Jiang, G., Hu, J., 2012, Integrated chemostratigraphy of the Doushantuo Formation at the north-ern Xiaofenghe section (Yangtze Gorges, South China) and its implication for Ediacaran stratigraphic correlation and ocean redox models: Precambrian Research, 192-195, 125-141. doi:10.1016/j.precamres.2011.10.021.
Zimmermann, U., Bahlburg, H., 2003, Provenance analysis and tectonic setting of the Ordovician clastic deposits in the southern Puna Basin, NW Argentina: Sedimentology, 50, 1079-1104. doi:10.1046/j.1365-3091.2003.00595.x.
Zimmermann, U., Poiré, D.G., Gómez Peral, L., 2011, Neoproterozoic to Lower Paleozoic successions of the Tandilia System in Argentina: implication for the paleotectonic framework of southwest Gondwana: International Journal of Earth Sicences, 100, 489-510. doi: 10.1007/s00531-010-0584-4.
Zuffa, G.G., 1985, Provenance of Arenites: Cosenza, North Atlantic Treaty Organization, Science Series C, 408 pp.

Manuscript received: June 16, 2015
Corrected manuscript received: September 6, 2015
Manuscript accepted: September 9, 2015